

DOI:10.1002/ejic.201301423

## 3,4-Ferrocenyl-Functionalized Pyrroles: Synthesis, Structure, and (Spectro)Electrochemical Studies

Marcus Korb,<sup>[a]</sup> Ulrike Pfaff,<sup>[a]</sup> Alexander Hildebrandt,<sup>[a]</sup> Tobias Rüffer,<sup>[a]</sup> and Heinrich Lang<sup>\*[a]</sup>

**Keywords:** Metallocenes / Alkynes / Heterocycles / Electrochemistry / Electron transfer

The synthesis of 3,4-diferrocenyl-substituted pyrroles of the type 3,4-Fc<sub>2</sub>-cC<sub>4</sub>H<sub>2</sub>NR [Fc = Fe(η<sup>5</sup>-C<sub>5</sub>H<sub>4</sub>)(η<sup>5</sup>-C<sub>5</sub>H<sub>5</sub>); R = Ph (**3a**), SO<sub>2</sub>-4-MeC<sub>6</sub>H<sub>4</sub> (Ts) (**3b**), SiPr<sub>3</sub> (**3c**)], 3,4-(FcC≡C)<sub>2</sub>-cC<sub>4</sub>H<sub>2</sub>NR [R = Ph (**4a**), Ts (**4b**)], and 3-Br-4-FcC≡C-cC<sub>4</sub>H<sub>2</sub>NR [R = Ph (**7a**), Ts (**7b**)] from 3,4-Br<sub>2</sub>-cC<sub>4</sub>H<sub>2</sub>NR [R = Ph (**2a**), Ts (**2b**), SiPr<sub>3</sub> (**2c**)] is discussed. The molecular structures of **3a**, **b**, **5**, **4b**, and **7b** in the solid state are reported and show that the formal double bonds in the heterocyclic core are

rather localized relative to pyrrole itself. The investigations with (spectro)electrochemical methods reveal the different capabilities for the formation of mixed-valent species and allows the classification of **3a**, **b** as class II systems, whereas compounds that feature electron-withdrawing -C≡C- units (**4a**, **b**) can be assigned to class I systems according to Robin and Day.

### Introduction

Recent investigations on diverse isomeric ferrocenyl-functionalized five-membered heterocycles including furan,<sup>[1,2]</sup> thiophene,<sup>[1,2]</sup> pyrrole,<sup>[1,2]</sup> phosphole,<sup>[3a]</sup> and maleimides,<sup>[3b,3c]</sup> as well as titana-<sup>[4]</sup> and zircona-cycles<sup>[5]</sup> as model compounds to explain the electronic communication across π-conjugated linking units in redox-active organometallic molecules have been performed, since these species can be understood as building blocks for electronic wires.<sup>[6,7]</sup> The 2,5-functionalization is the most investigated substitution pattern for heterocyclic compounds,<sup>[2,3,7-9]</sup> which is explainable by their straightforward accessibility. Super-crowded tetraferrocenyl five-membered heterocycles of thiophene and NR-pyrroles (R = Me, Ph) with their ferrocenyl substituents possess four reversible Fc/Fc<sup>+</sup> redox events, thus indicating that all ferrocenyl groups can be oxidized separately. The electrochemical and spectroelectrochemical (UV/Vis-NIR, IR spectroscopy) properties of these species were studied.<sup>[3,10]</sup> In particular, the electronic communication between the redox-active ferrocenyls, depending on the different substitution pattern, has been investigated on the example of thiophene-bridged systems. It was found that the degree of intermetallic interaction decreases from the 2,5- to the 2,3-, 2,4-, and 3,4-functionalization.<sup>[11]</sup> Nevertheless, the differences, especially within the electrochemical data, between the different substitution pat-

terns are rather low, as the variety in resonance stabilization is compensated by the different electrostatic repulsion energies for the individual isomers.

(Spectro)electrochemical measurements within a series of furan-, thiophene-, pyrrole-, and phosphole-based ferrocenyl-functionalized systems confirmed that electron-rich heterocycles, such as methyl- and phenylpyrroles are best suited to promote electron transfer through the conjugated π system.<sup>[6,10]</sup> In this respect, we herein present the synthesis, characterization, and (spectro)electrochemical behavior of novel 3,4-functionalized 3,4-Fc<sub>2</sub>-cC<sub>4</sub>H<sub>2</sub>NR [Fc = Fe(η<sup>5</sup>-C<sub>5</sub>H<sub>4</sub>)(η<sup>5</sup>-C<sub>5</sub>H<sub>5</sub>); R = Ph, Ts, SiPr<sub>3</sub>] and 3,4-(FcC≡C)<sub>2</sub>-cC<sub>4</sub>H<sub>2</sub>NR (R = Ph, Ts), as these molecules exhibit both the less favored 3,4-substitution and the advantageous electron-rich pyrrole core. In addition, it could be demonstrated that the electronic behavior of the pyrrole unit itself is highly dependent on the electron-withdrawing or electron-donating character of the substituent R at nitrogen.<sup>[10]</sup> To confirm this influence in 3,4-substituted isomers, the phenyl and the electron-withdrawing tosyl functionality have been introduced.

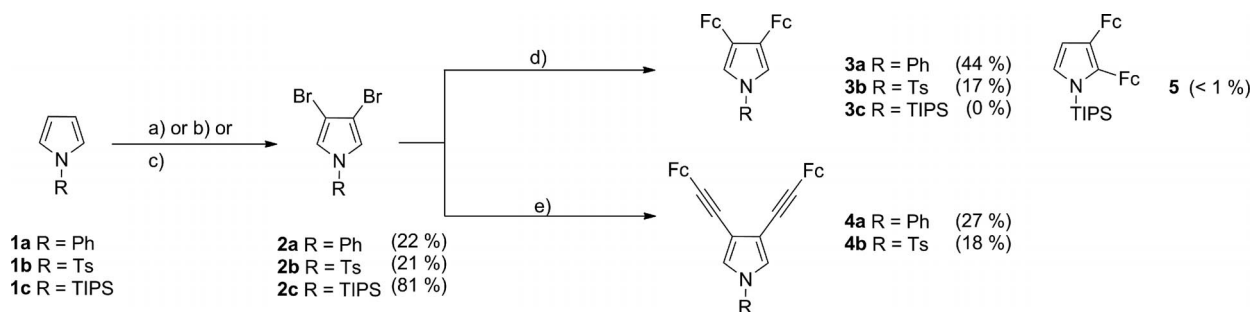
### Results and Discussion

#### Synthesis and Characterization

N-Substituted pyrroles **2-7** (Schemes 1 and 2) have been investigated to examine their steric and electronic properties. Therefore, 3,4-dibromopyrroles 3,4-Br<sub>2</sub>-cC<sub>4</sub>H<sub>2</sub>NR [R = Ph (**2a**), SO<sub>2</sub>-4-MeC<sub>6</sub>H<sub>4</sub> (Ts) (**2b**), SiPr<sub>3</sub> (**2c**)] were synthesized from cC<sub>4</sub>H<sub>4</sub>NR [R = Ph (**1a**), Ts (**1b**), SiPr<sub>3</sub> (**1c**)] by using different bromination reactions as outlined in Scheme 1.<sup>[12-14]</sup> For sterically less-demanding N-substitu-

[a] Technische Universität Chemnitz, Faculty of Natural Sciences, Institute of Chemistry, Inorganic Chemistry, 09107 Chemnitz, Germany  
E-mail: heinrich.lang@chemie.tu-chemnitz.de  
http://www.tu-chemnitz.de/chemie/anorg/

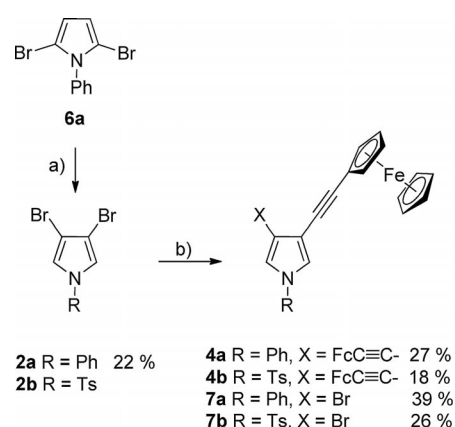
Supporting information for this article is available on the WWW under <http://dx.doi.org/10.1002/ejic.201301423>.



Scheme 1. Synthesis of 3,4-diferrocenyl-substituted pyrroles **3a,b**, **4a,b**, and **5**, respectively. (a) R = Ph: (1) NBS, tetrahydrofuran (THF),  $-80^{\circ}\text{C}$ ; (2) TsOH, acetonitrile, toluene,  $0 \rightarrow 25^{\circ}\text{C}$ , 16 h. (b) R = Ts: Br<sub>2</sub>, AcOH, reflux, 90 min. (c) R = TIPS: NBS, THF,  $-80^{\circ}\text{C}$ . (d) (1) FcZnCl,  $-80^{\circ}\text{C}$ ; (2) 1–0.25 mol-% [ $\{\text{Pd}[\text{CH}_2\text{C}(\text{CH}_3)_2\text{P}(\text{C}_4\text{H}_9)_2](\mu\text{-Cl})\}_2$ ],  $60^{\circ}\text{C}$ , **2a–c**. (e) [Cu], NH(*i*Pr)<sub>2</sub>, THF, PPh<sub>3</sub>, 1 mol-% [ $\text{PdCl}_2(\text{PPh}_3)_2$ ], FcC≡CH, 72 h,  $65^{\circ}\text{C}$ .

ents like the phenyl and tosyl group, respectively, treatment with either *N*-bromosuccinimide (NBS; synthesis of **2a**) or bromine (synthesis of **2b**) gave at first the respective 2,5-dibromo derivative 2,5-Br-*c*C<sub>4</sub>H<sub>2</sub>NR, which subsequently rearranges under acidic conditions to produce the thermodynamically more stable 3,4-isomers **2a** and **2b**, respectively (Scheme 1).<sup>[13]</sup> However, the sterically demanding Si*i*Pr<sub>3</sub> (TIPS) protecting group shields the 2,5-position of the pyrrole and hence selectively directs the substituents into the 3- and 4-positions even at  $-78^{\circ}\text{C}$ . It should be noted that higher yields can be obtained when working in the absence of light.<sup>[12,14]</sup> The introduction of either ferrocenyl or ferrocenylethynyl substituents is possible by palladium-catalyzed C–C cross-coupling reactions.<sup>[9,15]</sup> Treatment of **2a–c** with FcZnCl<sup>[9]</sup> using the Negishi coupling protocol in the presence of catalytic amounts of [ $\{\text{Pd}[\text{CH}_2\text{C}(\text{CH}_3)_2\text{P}(\text{C}_4\text{H}_9)_2](\mu\text{-Cl})\}_2$ ] afforded the 3,4-diferrocenyl-substituted pyrroles **3a** and **3b** as depicted in Scheme 1. Unfortunately, the TIPS-protected pyrrole **2c** did not convert to **3c** under the relatively high reaction temperatures as well as the basic reaction conditions applied, which is in accordance with other reported reactions using **2c** as the starting material.<sup>[16]</sup> After column chromatography only a small amount (<1%; Exp. Sect.) of a soluble material could be recovered. Mass spectrometric studies showed the molecular-ion peak corresponding to Fc<sub>2</sub>-*c*C<sub>4</sub>H<sub>2</sub>*N*-TIPS<sup>+</sup>. Nevertheless, by hand-picking, single crystals could be separated, which enabled us to carry out a single-crystal X-ray structure determination that demonstrated the formation of the constitution isomer 2,3-diferrocenylpyrrole *N*-TIPS (**5**) (Scheme 1). The formation of **5** from **2c** can be explained by a metal–halogen exchange reaction during the catalytic process.<sup>[17]</sup>

For the synthesis of the respective ferrocenylethynyl-functionalized compounds **7a** and **7b** (Scheme 2), the Sonogashira C–C cross-coupling protocol was applied.<sup>[15]</sup> Thus, the reaction of pyrroles **2a** and **2b** with FcC≡CH gave the bis(ferrocenylethynyl)-substituted pyrroles **4a** and **4b**, which could be separated after appropriate workup in yields between 18–27% (Scheme 1; Exp. Sect.). However, during the synthesis of **4a,b**, the mono-ferrocenylethynyl-substituted compounds 3-Br-4-FcC≡C-*c*C<sub>4</sub>H<sub>2</sub>NR [R = Ph (**7a**), Ts (**7b**)] were additionally formed. Hence, purification methods including column chromatography and crystallization pro-



Scheme 2. Synthesis of 3,4-diferrocenylethynyl-substituted pyrroles **4a** and **4b** and the mono-ferrocenylethynyl-substituted pyrroles **7a** and **7b**. (a) TsOH, toluene/acetonitrile (ratio 1:1, v/v),  $0^{\circ}\text{C} \rightarrow 25^{\circ}\text{C}$ . (b) FcC≡CH, 1 mol-% [ $\text{PdCl}_2(\text{PPh}_3)_2$ ], THF, NH(*i*Pr)<sub>2</sub>,  $65^{\circ}\text{C}$ , 72 h.

cedures had to be carried out (see the Exp. Sect.). This decisively lowered the yield of the main products **4a,b**. It should be noted that using different stoichiometries or temperatures did not significantly influence the ratio of the product formation.

Organometallic compounds **3**, **4**, and **7** are orange solid materials, which are stable to air and moisture for months. They are soluble in most common organic solvents including toluene, dichloromethane, THF, and boiling *n*-hexane. They have been characterized by elemental analysis, IR, and NMR (<sup>1</sup>H, <sup>13</sup>C{<sup>1</sup>H}) spectroscopy, and ESI-TOF mass spectrometry (see the Exp. Sect.). The electrochemical and spectroelectrochemical properties of **3a,b** and **4a,b** were determined by cyclic voltammetry (CV), square-wave voltammetry (SWV), and in situ UV/Vis-NIR as well as IR spectroscopy.

The <sup>1</sup>H NMR spectra of **3a,b**, **4b**, and **7b** display one sharp singlet for the η<sup>5</sup>-bonded cyclopentadienyl groups C<sub>5</sub>H<sub>5</sub> and two pseudotriplets (<sup>3,4</sup>J<sub>H,H</sub> = 1.9 Hz) for the protons of the respective C<sub>5</sub>H<sub>4</sub> ligands as characteristic for an AA'XX' spin system.<sup>[18]</sup> The α-hydrogen atoms at the pyrrole core give rise to one singlet for the symmetrical functionalized species at δ = 7.18 ppm for **3a** and **4a**, δ =

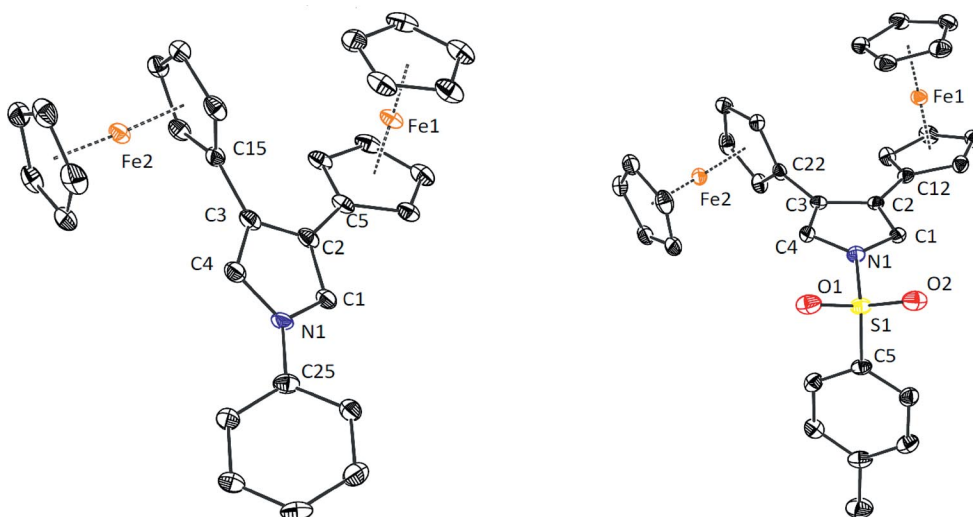


Figure 1. ORTEP diagram (50% probability level) of the molecular structure of **3a** (left) and **3b** (right) with the atom-numbering scheme. Hydrogen atoms have been omitted for clarity. Selected bond lengths [Å], angles [°], and torsion angles [°]: Compound **3a**: C1–C2 1.375(5), C2–C3 1.441(5), C3–C4 1.370(5), average N–C 1.37(10), C2–C5 1.455(5), C3–C15 1.474(5), D1–Fe1 1.6565(5), D2–Fe1 1.6497(6), D3–Fe2 1.6567(6), D4–Fe2 1.6574(6), N1–C25 1.426(5); C4–N1–C1 107.9(3), D1–Fe1–D2 177.88(4), D3–Fe2–D4 176.89(4), C26–C25–N1–C1 –147.5(4), C1–C2–C5–C6 151.2(4), C4–C3–C15–C16 65.4(5), C5–D1–D2–C10 2.4(3), C15–D3–D4–C20 –10.9(3), average Fe–Fe 6.0287. Compound **3b**: C1–C2 1.371(3), C2–C3 1.458(3), C3–C4 1.356(3), average N–C 1.389(6), N1–S1 1.662(2), C2–C12 1.458(3), C3–C22 1.473(3), D1–Fe1 1.643(2), D2–Fe1 1.652(2), D3–Fe2 1.652(2), D4–Fe2 1.653(2), Fe1–Fe2 6.0313(9); C4–N1–C1 108.99(19), C1–C2–C12 124.3(2), C4–C3–C22 124.8(2), D1–Fe1–D2 177.61(2), D3–Fe2–D4 178.15(2), C1–N1–S1–C5 –76.13(21), C4–C3–C22–C23 76.51(32), C1–C2–C12–C13 –19.0(4), C12–D1–D2–C17 6.11(17), C22–D3–D4–C27 –25.22(16). D1 and D3 denote the centroid of C<sub>5</sub>H<sub>4</sub>; D2 and D4 denote the centroid of C<sub>5</sub>H<sub>5</sub>.

7.12 ppm for **3b**, and  $\delta = 7.27$  ppm for **4b** as well as two doublets for the unsymmetrical systems at  $\delta = 7.07$  and 7.24 ppm for **7a** and  $\delta = 7.16$  and 7.28 ppm for **7b**. This indicates that the substituents R at the nitrogen atom do have a direct influence on the chemical shift of the  $\alpha$  protons. In addition, with the electron-withdrawing groups –C≡C– and Br in positions 3 and 4, the signal is either shifted to higher (**3b**) or lower (**4b**) field. The shift of the C<sub>5</sub>H<sub>5</sub> ring protons is also primarily influenced by the substituents in the 3- and 4-position.

The IR spectra of **4** and **7** show a characteristic  $\nu_{(C=C)}$  absorption at 2208 (**4a**), 2215 (**4b**), 2240 (**7a**), and 2223 cm<sup>-1</sup> (**7b**) for the ferrocenylethynyl units, which is typical for this type of building block.<sup>[19]</sup>

The molecular structures of **3a,b**, **4b**, **5**, and **7b** in the solid state have been determined by single-crystal X-ray diffraction analysis (Figures 1, 2, and 3).

Suitable crystals were obtained either by slow diffusion of methanol into a solution of the respective organometallic compound in dichloromethane or by crystallization from *n*-hexane solutions at low temperature (see the Exp. Sect.). In addition, the structures of pyrroles **1b**, **2b**, and **2c**<sup>[12]</sup> in the solid state are given in Figures S7–S9 of the Supporting Information. Important bond lengths [Å], bond angles [°], and torsion angles [°] are summarized in the captions of Figures 1, 2, and 3. For crystal and structure refinement data, see the Supporting Information.

Compounds **3b**, **4b**, and **7b** crystallize in the triclinic space group *P* $\bar{1}$  with one crystallographically independent molecule in the asymmetric unit, whereas **3a** and **5** crystallize in the monoclinic space groups *P2*/*c* (**3a**) or *P2*<sub>1</sub>/*n* (**5**)

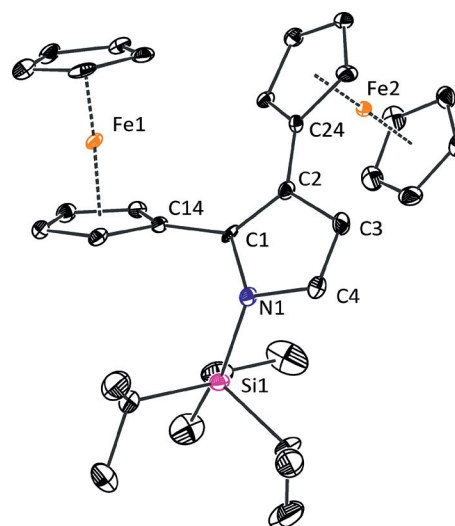


Figure 2. ORTEP diagram (50% probability level) of the molecular structure of **5** with the atom-numbering scheme. All hydrogen atoms have been omitted for clarity. Selected bond lengths [Å], angles [°], and torsion angles [°]: C1–N1 1.424(4), C1–C2 1.378(5), C2–C3 1.428(5), C3–C4 1.352(5), C4–N1 1.387(4), N1–Si1 1.794(3), C1–C14 1.477(5), C2–C24 1.473(5), D1–Fe1 1.6487(5), D2–Fe1 1.6484(5), D3–Fe2 1.6384(5), D4–Fe2 1.6416(5); N1–C1–C14 118.5(3), C3–C2–C24 122.1(3), C1–N1–C4 106.0(3), D1–Fe1–D2 177.03(3), D3–Fe2–D4 178.79(3), N1–C1–C14–C15 47.44(5), C3–C2–C24–C25 –23.8(5), C14–D1–D2–C19 1.1(3), C24–D3–D4–C30 –8.0(3); average Fe–Fe 5.6709. D1 and D3 denote the centroid of C<sub>5</sub>H<sub>4</sub>; D2 and D4 denote the centroid of C<sub>5</sub>H<sub>5</sub>.

with two (**3a**) or three (**5**) crystallographically independent molecules in the asymmetric unit. 3,4-Diferrocenyl-substi-

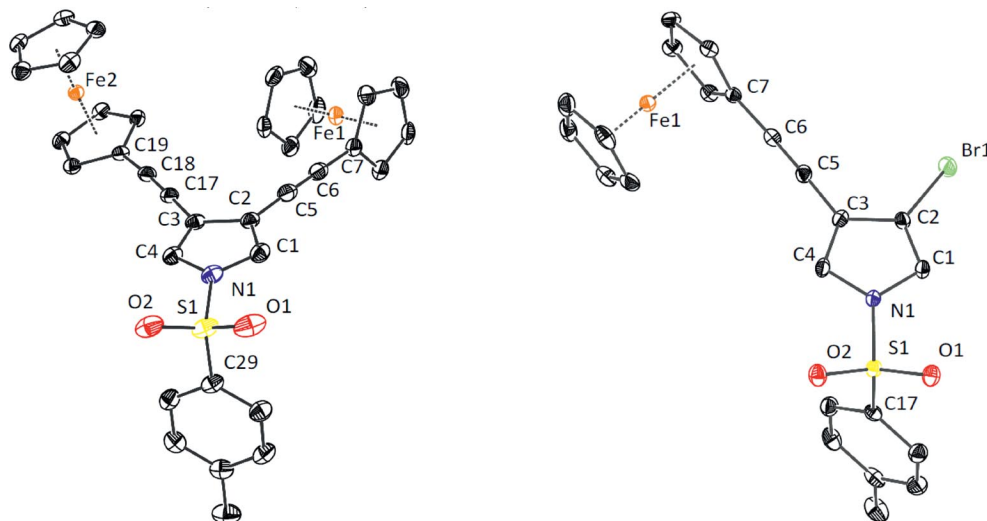


Figure 3. ORTEP diagram (50% probability level) of the molecular structure of **4b** (left) and **7b** (right) with the atom-numbering scheme. All hydrogen atoms have been omitted for clarity. Selected bond lengths [Å], angles [°], and torsion angles [°]: Compound **4b**: C1–C2 1.370(3), C2–C3 1.446(3), C3–C4 1.367(3), average N–C 1.387(6), N1–S1 1.6722(17), C2–C5 1.422(3), C3–C17 1.437(3), C5–C6 1.210(3), C6–C7 1.417(3), C17–C18 1.194(3), C18–C19 1.419(3), D1–Fe1 1.6444(3), D2–Fe1 1.6450(3), D3–Fe2 1.6446(3), D4–Fe2 1.6536(3), Fe1–Fe2 7.2153(5), C2–C5–C6 177.7(2), C5–C6–C7 179.6(3), C4–N1–C1 108.99(19), C3–C17–C18 177.5(2), C17–C18–C19 175.4(2), D1–Fe1–D2 179.01(2), D3–Fe2–D4 178.74(2), C1–N1–S1–C29 –83.45(18), C12–D1–D2–C17 –3.10(14), C19–D3–D4–C24 –9.18(14). Compound **7b**: C1–C2 1.354(3), C2–C3 1.436(3), C3–C4 1.368(3), C2–Br1 1.868(2), C3–C5 1.436(3), C5–C6 1.188(3), C6–C7 1.432(3), average N–C 1.393(6), N1–S1 1.6769(19), D1–Fe1 1.6433(4), D2–Fe1 1.6489(4), C4–N1–C1 109.56(18), C6–C5–C3 176.3(3), C5–C6–C7 177.7(2), D1–Fe1–D2 179.26(2), C1–N1–S1–C17 80.3(2), C7–D1–D2–C12 2.46(16) [D1 (and D3) denotes the centroid of C<sub>5</sub>H<sub>4</sub>; D2 (and D4) denotes the centroid of C<sub>5</sub>H<sub>5</sub>].

tuted pyrroles contain one orthogonally positioned [**3a**, 69.04(14)°; **3b**, 77.98(9)°, **4b**, 82.25(7)°, **7b**, 83.55(10)°] and one rather coplanar-oriented ferrocenyl unit [**3a**, 27.5(2)°; **3b**, 19.85(14)°, **4b**, 11.73(14)°]. In the 2,3-disubstituted compound **5**, the steric interaction of the ferrocenyl substituents with the *N*-triisopropylsilyl moieties results in a torsion angle of 47.44(5)°. The substituent in position 3 is rotated by 26.44(19)° from coplanarity with the five-membered *N*-heterocyclic core. The torsion angles of the ferrocenyls themselves are rather staggered [**3b**, –25.22(16)°] or deviate slightly from an eclipsed conformation (Figures 1, 2, and 3). With regard to the iron–iron distances, the values increase from the 2,3-substituted compound **5** (average of three molecules: 5.67 Å) through the 3,4-diferrocenyl-substituted pyrroles **3a** and **3b** (**3a**, 6.03 Å; **3b**, 6.03 Å) to **4b** (7.22 Å) with two additional ethynyl moieties.

The aromaticity of the pyrroles can be compared by calculating the  $\tau$  parameter, which describes the difference between carbon–carbon single and carbon–carbon double bonds (Table 1).<sup>[9,20]</sup>

In comparison to tetraferrocenylpyrrole<sup>[2]</sup> (TFP) and unsubstituted 1*H*-pyrrole, which show high  $\tau$  parameters and thus a high aromaticity,<sup>[2,20]</sup> all reported ferrocenyl(ethynyl)-substituted molecules possess a larger bond length alternation (Table 1). For all newly prepared compounds within this study, the C1–C2 and C3–C4 distances are significantly decreased relative to TFP with the exception of **3a** (Table 1). Interestingly, the C2–C3 as well as the C–N distances are almost entirely unaffected. Only for unsymmetric **5** is the C1–N1 bond length increased owing to a steric interaction with the *N*-triisopropylsilyl moiety.

Table 1. Selected bond lengths [Å] and  $\tau$  parameters of 2,3,4,5-tetraferrocenyl-*N*-phenylpyrrole (TFP) for comparison with **3a**, **4b**, **5**, and **7b**.

	$\tau$ <sup>[a]</sup>	N1–C1	N1–C4	C1–C2	C2–C3	C3–C4
TFP	0.832	1.393(3)	1.394(3)	1.400(3)	1.435(3)	1.386(3)
<b>3a</b>	0.678	1.374(5)	1.375(5)	1.375(5)	1.441(5)	1.370(5)
<b>3b</b>	0.575	1.391(3)	1.387(3)	1.371(3)	1.458(3)	1.356(3)
<b>4b</b>	0.628	1.384(3)	1.389(3)	1.370(3)	1.446(3)	1.367(3)
<b>5</b>	0.757	1.424(4)	1.387(4)	1.378(5)	1.428(5)	1.352(5)
<b>7b</b>	0.667	1.396(3)	1.389(3)	1.354(3)	1.436(3)	1.368(3)

[a]  $\tau$ (1*H*-pyrrole) = 0.830.<sup>[2,20]</sup>

### (Spectro)Electrochemical Studies

The redox properties of **3a**, **4a**, **4b**, and **7b** were determined by CV, SWV (Figure 4) and in situ UV/Vis-NIR and IR spectroscopy (Figure 5 and Figures S1–S5 in the Supporting Information). Solutions of the analyte (1.0 mmol L<sup>–1</sup>) in dichloromethane with [N*n*Bu<sub>4</sub>][B(C<sub>6</sub>F<sub>5</sub>)<sub>4</sub>] (0.1 mol L<sup>–1</sup>)<sup>[9,21–23,24]</sup> as supporting electrolyte were used. The data of the CV measurements have been recorded at a scan rate of 100 mV s<sup>–1</sup> and are summarized in Table 2.

All redox potentials are referenced to the FcH/FcH<sup>+</sup> redox couple [ $E^{\circ'} = 0.00$  mV, FcH = Fe( $\eta^5$ -C<sub>5</sub>H<sub>5</sub>)<sub>2</sub>].<sup>[25]</sup>

Figure 4 shows the cyclic and square-wave voltammograms of **3a**, **4a**, **4b**, and **7b**. For **3a**, **4a**, **4b**, and **7b** two reversible redox events that correspond to the two ferrocenyl sandwich units were detected. Owing to the electron-withdrawing character of the tosyl substituent in **3b**, the electron density in the pyrrole core is less than in **3a**, which is reflected by the

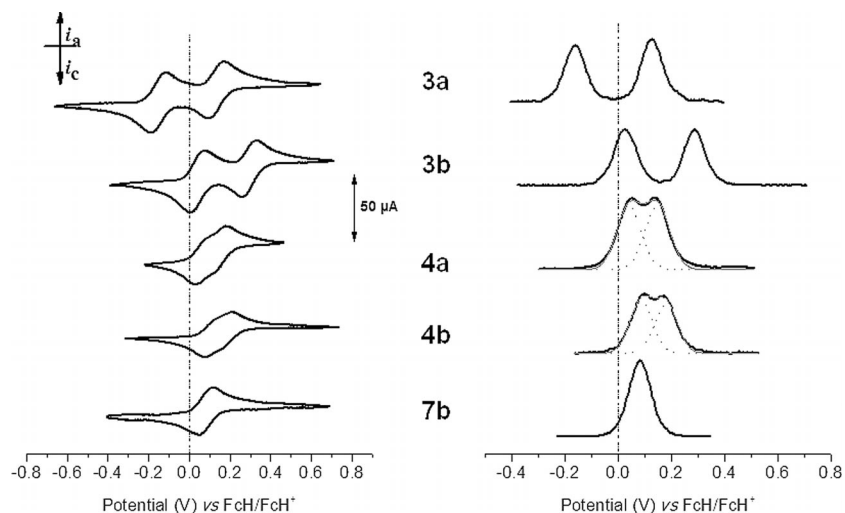


Figure 4. Voltammograms of solutions of 1.0 mmol L<sup>-1</sup> of **3a,b**, **4a,b**, and **7b** in dichloromethane at 25 °C. Supporting electrolyte [N(*n*Bu)<sub>4</sub>][B(C<sub>6</sub>F<sub>5</sub>)<sub>4</sub>] (0.1 mol L<sup>-1</sup>). Left: Cyclic voltammograms (scan rate: 100 mV s<sup>-1</sup>). Right: Square-wave voltammograms (scan rate: 1 mV s<sup>-1</sup>).

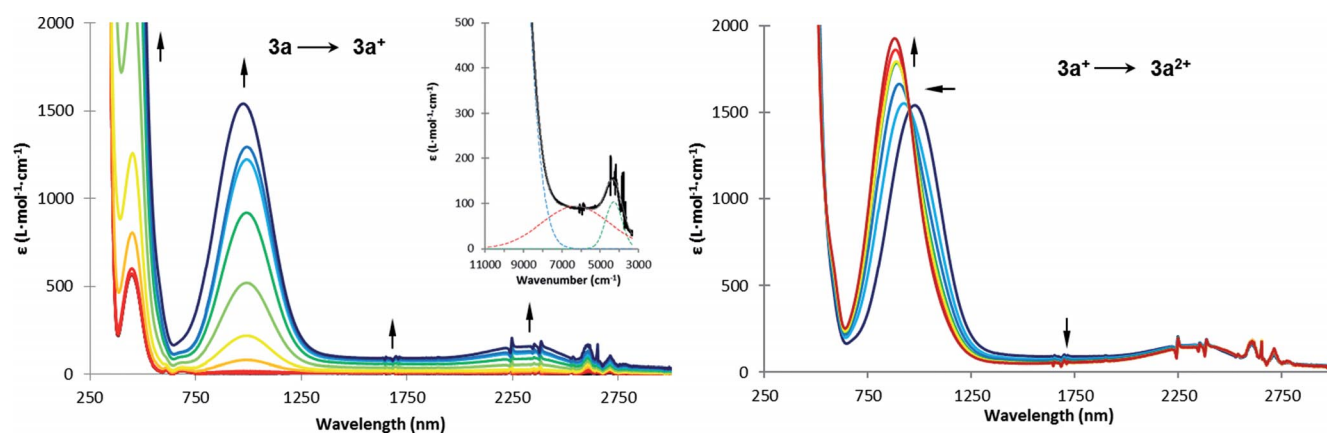


Figure 5. UV/Vis-NIR spectra of **3a** at rising potentials versus Ag/AgCl: -200–300 mV (left), 300–1000 mV (right). Inset: Deconvolution of the NIR absorptions at 300 mV of in situ generated **3a<sup>+</sup>** using three Gaussian-shaped bands. Measurement conditions: 25 °C, dichloromethane, 0.1 mol L<sup>-1</sup> [N(*n*Bu)<sub>4</sub>][B(C<sub>6</sub>F<sub>5</sub>)<sub>4</sub>] as supporting electrolyte.

Table 2. Cyclic voltammetry data of **3a,b**, **4a,b**, and **7b**.<sup>[a]</sup>

	$E_1^{o'}$ [mV] <sup>[b]</sup> ( $\Delta E_p$ [mV]) <sup>[c]</sup>	$E_2^{o'}$ [mV] <sup>[b]</sup> ( $\Delta E_p$ [mV]) <sup>[c]</sup>	$\Delta E^{o'}$ [mV] <sup>[d]</sup>
<b>3a</b>	-150 (72)	135 (74)	285
<b>3b</b>	40 (70)	295 (66)	255
<b>4a</b>	105 (146)	–	110 <sup>[e]</sup>
<b>4b</b>	140 (132)	–	95 <sup>[e]</sup>
<b>7b</b>	80 (69)	–	–

[a] Potentials versus FcH/FcH<sup>+</sup> (scan rate 100 mV s<sup>-1</sup>) at a glassy-carbon electrode of 1.0 mmol L<sup>-1</sup> solutions of the analytes in dichloromethane that contained 0.1 mol L<sup>-1</sup> of [N(*n*Bu)<sub>4</sub>][B(C<sub>6</sub>F<sub>5</sub>)<sub>4</sub>] as supporting electrolyte at 25 °C. [b]  $E^{o'}$  = formal potential. [c]  $\Delta E_p$  = difference between the oxidation and the reduction potential. [d]  $\Delta E^{o'}$  = potential difference between the two ferrocenyl-related redox processes. [e] Determined using deconvolution of the redox separation of the oxidation potentials in SWV (Figure 4) and the method of Richardson and Taube.<sup>[24]</sup>

higher  $E_1^{o'}$  value [-150 (**3a**), 40 mV (**3b**); Table 2]. The lower electron density in the heterocyclic unit relative to **3a**

leads to a smaller redox separation ( $\Delta E^{o'} = 255$  mV) for **3b**. A similar behavior has been observed for other ferrocenyl-functionalized five-membered heterocycles.<sup>[6]</sup> When the iron–iron distance is increased by additional –C≡C– linking units, as given in **4a,b**, the redox separation decreases significantly. The cyclic voltammogram (Figure 4) shows two individual one-electron processes for the oxidation of both ferrocenyl termini, which take place in a close potential range. Considering the redox processes as single reversible wave, high  $\Delta E_p$  values [146 (**4a**), 132 mV (**4b**)] were determined, which suggests two individual one-electron events. The deconvolution of the square-wave voltammograms gives a small redox separation of  $\Delta E^{o'} = 110$  (**4a**) and 95 mV (**4b**), respectively. Richardson and Taube presented another method in which the  $\Delta E^{o'}$  value can be estimated by calculation of the signal width at half of the maximum current within the square-wave voltammogram.<sup>[24]</sup> The application of both methods gives similar redox splittings between the individual ferrocenyl-related oxidation processes.

As expected, complex **7b** shows only one reversible redox process at  $E_1^{o'} = 80$  mV for the oxidation of the single metal center.

Comparison of **3a** with 2,5-diferrocenyl-*N*-phenylpyrrole<sup>[6,9]</sup> ( $\Delta E^{o'} = 450$  mV, [N(*n*Bu)<sub>4</sub>][B(C<sub>6</sub>F<sub>5</sub>)<sub>4</sub>] as supporting electrolyte) indicates that the position of the ferrocenyl substituents at the five-membered heterocyclic core has a strong influence on the redox separation and electronic coupling, respectively. Owing to the ferrocenyls in position 3 and 4 (**3a**), an oxidation of the ferrocenyl ligands at more anodic potentials is typical. The redox separation itself can be divided into different contributing factors: the electrostatic contribution ( $\Delta E_c$ ), the synergistic contribution ( $\Delta E_s$ ), the statistical contribution (36 mV), and the contribution caused by resonance stabilization ( $\Delta E_r$ ) of which only the latter is related to electron-transfer interactions [Equation (1)].

$$\Delta E^{o'} = \Delta E_c + \Delta E_s + 36 \text{ mV} + \Delta E_r \quad (1)$$

For a series of 2,5-diferrocenyl-functionalized five-membered heterocycles,<sup>[2,6]</sup> it could be shown that under the applied measurement conditions the sum of the electrostatic contribution ( $\Delta E_c$ ), the synergistic contribution ( $\Delta E_s$ ), and the statistical contribution (36 mV) has been determined to 209 mV, whereas the resonance stabilization energy depends on the corresponding heterocycle.<sup>[6]</sup> It can be assumed that within the five-membered heterocyclic molecules with ferrocenyl groups in the 3,4-position, the electrostatic contribution is larger than for the appropriate 2,5-isomers owing to the spatial proximity of the redox-active termini. On the example of diferrocenyl thiophenes (2,5- and 3,4-position), it was shown that the larger electrostatic term partially compensates the lower resonance stabilization to result in similar  $\Delta E^{o'}$  values for both isomers (3,4-diferrocenyl thiophene,  $\Delta E^{o'} = 244$  mV; 2,5-diferrocenyl thiophene,  $\Delta E^{o'} = 260$  mV).<sup>[6,11]</sup> Nevertheless, the electron-transfer interaction observed within the 2,5-diferrocenyl-*N*-phenylpyrrole is much larger relative to the respective thiophene analogue.<sup>[2]</sup> The drop within the redox separation from 450 mV for the 2,5-isomer towards 285 mV for the 3,4-isomer (**3a**) (Figure 4) emphasizes that the electronic interaction also decreases by a great amount.

By using only electrochemical measurements, it cannot be estimated if electron transfer is present in the mixed-valent molecules **3a,b**<sup>+</sup> and **4a,b**<sup>+</sup> or if the redox splitting is caused solely by electrostatic repulsion of the individual ferrocenium units. To gain a deeper insight into the electronic properties of the individual oxidation states of the latter compounds, in situ spectroelectrochemical UV/Vis-NIR and IR measurements were carried out. Spectroelectrochemical studies were performed by a stepwise increase of the potential (step heights: 15, 25, 50, or 100 mV) from -200 to 1000 mV versus Ag/AgCl in an optically transparent thin-layer electrochemistry (OTTLE) cell<sup>[26]</sup> by using solutions of **3a,b** and **4a,b** (0.005 mol L<sup>-1</sup>) in dichloromethane that contained [N*n*Bu<sub>4</sub>][B(C<sub>6</sub>F<sub>5</sub>)<sub>4</sub>] (0.1 mol L<sup>-1</sup>) as electrolyte at 25 °C. During this procedure, **3a,b** and **4a,b** were oxidized to the mixed-valent species **3a,b**<sup>+</sup> and **4a,b**<sup>+</sup> and

finally to dicationic **3a,b**<sup>2+</sup> and **4a,b**<sup>2+</sup>, respectively (Figure 5 and Figures S1–S5 in the Supporting Information). For **3a**, within successive oxidation, increasing absorptions at the edge of the UV/Vis (980 nm) and NIR (2310 nm) region could be observed, which can be assigned to ligand-to-metal charge transfer (LMCT), involving the pyrrolic spacer unit,<sup>[21]</sup> and ligand-field (LF) transitions (Figure 5). The forbidden metal-centered ligand-field (LF) electronic transition usually occurs at approximately 4000 cm<sup>-1</sup> with a very low intensity (generally close to 100 L mol<sup>-1</sup> cm<sup>-1</sup>) (Figure 5).<sup>[27,28]</sup> The LMCT and LF transition can be described very well by Gaussian-shaped functions by using the method of deconvolution (Figure 5). Considering that the experimental graph is described by two Gauss functions (Table 3), the extinction should tend to zero in the region between 5000 and 7000 cm<sup>-1</sup>. However, the experimental curve has an extinction of  $\epsilon_{\text{max}} = 95$  L mol<sup>-1</sup> cm<sup>-1</sup> within this part, which prompted us to apply a third Gaussian-shaped function to the simulation.

Table 3. NIR data of **3a**<sup>+</sup> and **3b**<sup>+</sup>.<sup>[a]</sup>

	Transition	$\tilde{\nu}_{\text{max}}$ [cm <sup>-1</sup> ]	$\epsilon_{\text{max}}$ (L mol <sup>-1</sup> cm <sup>-1</sup> )	$\Delta\nu_{1/2}$ [cm <sup>-1</sup> ]
<b>3a</b> <sup>+</sup>	LF <sup>[b]</sup>	4290	100	1025
	IVCT	6285	95	4165
	LMCT	10090	1620	2270
<b>3b</b> <sup>+</sup>	LF <sup>[b]</sup>	4170	65	2255
	IVCT	7210	65	4115
	LMCT	11720	680	2615

[a] In dry dichloromethane containing 0.1 mol L<sup>-1</sup> of [N*n*Bu<sub>4</sub>][B(C<sub>6</sub>F<sub>5</sub>)<sub>4</sub>] as supporting electrolyte at 25 °C. [b] Ligand-field transition.

The new band shows typical characteristics of an intervalence charge-transfer (IVCT) transition for the mixed-valent species **3a**<sup>+</sup> with a very small extinction ( $\epsilon_{\text{max}} = 95$  L mol<sup>-1</sup> cm<sup>-1</sup>,  $\tilde{\nu}_{\text{max}} = 6285$  cm<sup>-1</sup>,  $\Delta\nu_{1/2} = 4165$  cm<sup>-1</sup>). The obtained values should be handled with care, as the simulation of this band is solely based on the extinction within this region, which causes the  $\Delta\nu_{1/2}$  in particular to be susceptible to errors. The band-shape analysis of the absorption in the NIR region of compound **3b** leads to a very broad IVCT band with low intensity (Table 3, Figure S1 in the Supporting Information). Nevertheless, the predictions of small intramolecular interactions in **3a,b** discussed within the electrochemical section (see above) are validated by these results. A low contribution of resonance stabilization energy causes a small and broad IVCT excitation. With this in mind, 3,4-diferrocenyl-*N*-phenylpyrrole (**3a**) and 3,4-diferrocenyl-*N*-tosylpyrrole (**3b**) could be classified as weak coupled class II systems according to Robin and Day.<sup>[29]</sup> Hence spectroelectrochemical investigations show the influence of the position of ferrocenyl groups on the intervalence charge transfer through the *N*-phenylpyrrole, thus demonstrating that the 2,5-position is more suitable to facilitate electron transfer.<sup>[25,28,30]</sup>

Molecules **4a,b** show similar but weaker absorptions for the LMCT [970 (**4a**), 860 nm (**4b**)] and LF [2425 (**4a**), 2500 nm (**4b**)] transitions (Figures S2–S3 in the Supporting

Information). The absorptions in the UV/Vis region (250–750 nm) include the  $\pi$ – $\pi^*$  of the pyrrole as well as the d–d transitions of the Fc substituents.<sup>[31]</sup> With the deconvolution method no IVCT transitions could be found. The additional –C≡C– spacer unit between the Fc and the pyrrole does not permit an electron transfer between the two metals over the pyrrole core in the mixed-valent species in **4a,b**. The spectroelectrochemical investigations confirm the results of the electrochemical measurements, and the redox separations [ $\Delta E^\circ = 110$  (**4a**), 95 mV (**4b**)] are mainly caused by synergistic and statistical contributions as well as electrostatic repulsion. Hence **4a,b** can be assigned to class I systems according to Robin and Day.<sup>[29]</sup>

The –C≡C– units in **4a** and **4b** allow further investigation by using in situ IR spectroelectrochemistry. Whereas measurements in KBr revealed weak –C≡C– stretching vibrations at 2208 (**4a**) and 2215  $\text{cm}^{-1}$  (**4b**), the less sensitive measurement conditions within an OTTLE cell<sup>[30]</sup> did not allow the detection of these bands. During the oxidation process of **4a** (from –200 to 575 mV) the characteristic  $\nu_{\text{C}\equiv\text{C}}$  vibration develops at 2195  $\text{cm}^{-1}$  owing to the in situ generation of mixed-valent **4a<sup>+</sup>** (Table 4, Figure S4 in the Supporting Information). The intensity of this absorption decreases upon further oxidation (**4a<sup>+</sup>** → **4a<sup>2+</sup>**) and is shifted to 2175  $\text{cm}^{-1}$ . Within the successive oxidation of **4b** an IR band at 2208  $\text{cm}^{-1}$  could be observed. With rising potential a gradual increase of the intensity of this band was found, which is attributed to the low thermal stability of **4b<sup>+</sup>**, thereby resulting in the successive formation of **4b<sup>2+</sup>**. These results correspond well with the UV/Vis-NIR measurements as they underpin the difference in the stability of **4a<sup>+</sup>** and **4b<sup>+</sup>**, respectively.

Table 4. Spectroelectrochemical IR data for **4a<sup>n+</sup>** and **4b<sup>n+</sup>** ( $n = 0, 1, 2$ ).

	$\nu_{\text{C}\equiv\text{C}}$ [ $\text{cm}^{-1}$ ] ( $n = 0$ ) <sup>[a]</sup>	$\nu_{\text{C}\equiv\text{C}}$ [ $\text{cm}^{-1}$ ] ( $n = 1$ )	$\nu_{\text{C}\equiv\text{C}}$ [ $\text{cm}^{-1}$ ] ( $n = 2$ )
<b>4a<sup>n+</sup></b>	2208	2195	2175
<b>4b<sup>n+</sup></b>	2215	–	2208

[a] Data collected from IR measurements (KBr) at ambient temperature.

## Conclusion

The 3,4-ferrocenyl-substituted pyrroles 3,4-Fc<sub>2</sub>-c-C<sub>4</sub>H<sub>2</sub>NR [Fc = Fe( $\eta^5$ -C<sub>5</sub>H<sub>4</sub>)( $\eta^5$ -C<sub>5</sub>H<sub>5</sub>); R = Ph (**3a**), Ts (**3b**), Si*i*Pr<sub>3</sub> (**3c**)] and the 3,4-bis(ferrocenylethynyl)-substituted pyrroles 3,4-(FcC≡C)<sub>2</sub>-c-C<sub>4</sub>H<sub>2</sub>NR [R = Ph (**4a**), Ts (**4b**)] were synthesized from the corresponding dibromo species 3,4-Br<sub>2</sub>-c-C<sub>4</sub>H<sub>2</sub>NR [R = Ph (**2a**), Ts (**2b**), Si*i*Pr<sub>3</sub> (**2c**)] using either Negishi (using FcZnCl chloride as reagent), or Sonogashira (with FcC≡CH) C–C cross-coupling protocols. The structures of **3a,b**, **4b**, **5**, and **7b** in the solid state were determined by single-crystal X-ray structure analysis. In contrast to unsubstituted pyrroles, 2,5-substituted, and oligo-pyrroles,<sup>[2,21]</sup> the newly synthesized 3,4-diferrocenyl- and 3,4-diferrocenylethynyl-substituted pyrroles showed a

low degree of delocalization between the formal C–C double and C–C single bonds. The redox properties of **3a,b**, **4a,b**, and **7b** using different (spectro)electrochemical methods were studied. Whereas the difference in the redox splitting between the appropriate 2,5- and 3,4-isomers is quite low for diferrocenyl thiophenes (2,5-isomer, 260 mV; 3,4-isomer, 244 mV),<sup>[6,11]</sup> within the appropriate diferrocenyl-substituted pyrroles, the  $\Delta E^\circ$  values are highly dependent on the substitution pattern (2,5-isomer, 450 mV; 3,4-isomer, 285 mV). Furthermore, the substituent on the nitrogen atom also influences  $\Delta E^\circ$ , as the electron-withdrawing tosyl functionality leads to a decreased redox splitting of 255 mV. Spectroelectrochemical investigation on **3a,b** and **4a,b** showed that intervalence charge transfer is only observed for **3a,b**, thereby allowing its classification as a class II system, whereas **4a,b** can be assigned to class I systems according to Robin and Day.<sup>[29]</sup>

## Experimental Section

**General:** All reactions were carried out under an atmosphere of nitrogen using standard Schlenk techniques. THF and *n*-hexane were purified by distillation from sodium/benzophenone ketyl. Diethyl ether was purified by distillation from sodium. Dichloromethane, *N,N*-dimethylformamide, *N,N*-diisopropylamine, and acetonitrile were purified by distillation from calcium hydride.

**Reagents:** *n*BuLi (2.5 M solution in *n*-hexane), *t*BuLi (1.6 M solution in *n*-pentane), triisopropylsilyl chloride, ferrocene, KO*t*Bu, *N*-phenylpyrrole, *N*-bromosuccinimide, 4-methylbenzenesulfonic acid, 4-methylbenzenesulfonyl chloride, triphenylphosphane, and copper(I) iodide were purchased from commercial suppliers and used without further purification. Ethynylferrocene,<sup>[32]</sup> 1-tosyl-1*H*-pyrrole (**1b**),<sup>[33]</sup> *N*-TIPS-pyrrole (**1c**),<sup>[12]</sup> 3,4-dibromo-*N*-phenylpyrrole (**2a**),<sup>[13]</sup> 2,5-dibromo-*N*-phenylpyrrole (**6a**),<sup>[34]</sup> and [N(*n*Bu)<sub>4</sub>][B(C<sub>6</sub>F<sub>5</sub>)<sub>4</sub>]<sup>[22]</sup> were prepared according to published procedures. [ZnCl<sub>2</sub>·2thf] was obtained by drying ZnCl<sub>2</sub> with thionyl dichloride and the addition of THF. The palladium catalyst [{Pd[CH<sub>2</sub>C(CH<sub>3</sub>)<sub>2</sub>-P(*t*C<sub>4</sub>H<sub>9</sub>)<sub>2</sub>](μ-Cl)<sub>2</sub>] was synthesized according to Clark et al.,<sup>[35]</sup> and [PdCl<sub>2</sub>(PPh<sub>3</sub>)<sub>2</sub>] was synthesized according to Miyaura et al.<sup>[36]</sup>

**Instruments:** <sup>1</sup>H (500.3 MHz), <sup>13</sup>C{<sup>1</sup>H} (125.8 MHz), and <sup>29</sup>Si{<sup>1</sup>H} (99.4 MHz) NMR spectra were recorded with a Bruker Avance III 500 spectrometer operating at 298 K in the Fourier transform mode. Chemical shifts are reported in  $\delta$  [ppm] using deuterated solvent residues as internal standard ([D<sub>1</sub>]chloroform: <sup>1</sup>H at  $\delta = 7.26$  ppm and <sup>13</sup>C{<sup>1</sup>H} at  $\delta = 77.00$  ppm). Infrared spectra were recorded with an FTIR Nicolet IR 200 instrument. The melting points of analytically pure samples (sealed in nitrogen-purged capillaries) were determined with a Gallenkamp MFB 595 010 M melting point apparatus. Microanalyses were performed with a Thermo FLASH EA 1112 Series instrument. Spectroelectrochemical measurements were carried out in an OTTLE cell<sup>[26]</sup> (quartz windows for UV/Vis-NIR; CaF<sub>2</sub> windows for IR) from solutions in dichloromethane that contained 0.1 mol L<sup>-1</sup> of [N*n*Bu<sub>4</sub>][B(C<sub>6</sub>F<sub>5</sub>)<sub>4</sub>] as supporting electrolyte with a Varian Cary 5000 spectrometer. High-resolution mass spectra were performed with a micrOTOF QII Bruker Daltonics workstation.

**Electrochemistry:** Measurements on 1.0 mmol L<sup>-1</sup> solutions of the analytes in dry air-free dichloromethane that contained 0.1 mol L<sup>-1</sup> of [N*n*Bu<sub>4</sub>][B(C<sub>6</sub>F<sub>5</sub>)<sub>4</sub>] as supporting electrolyte were conducted under a blanket of purified argon at 25 °C with a Radiometer Voltalab

PGZ 100 electrochemical workstation interfaced with a personal computer. A three-electrode cell, which utilized a Pt auxiliary electrode, a glassy carbon working electrode (surface area 0.031 cm<sup>2</sup>), and an Ag/Ag<sup>+</sup> (0.01 mol L<sup>-1</sup> [AgNO<sub>3</sub>]) reference electrode mounted on a Luggin capillary. The working electrode was pre-treated by polishing on a Buehler microcloth first with a 1 μm and then with a 1/4 μm diamond paste. The reference electrode was constructed from a silver wire inserted into a solution of 0.01 mol L<sup>-1</sup> [AgNO<sub>3</sub>] and 0.1 mol L<sup>-1</sup> [N*n*Bu<sub>4</sub>][B(C<sub>6</sub>F<sub>5</sub>)<sub>4</sub>] in acetonitrile in a Luggin capillary with a vycor tip. This Luggin capillary was inserted into a second Luggin capillary with a vycor tip filled with a 0.1 mol L<sup>-1</sup> [N*n*Bu<sub>4</sub>][B(C<sub>6</sub>F<sub>5</sub>)<sub>4</sub>] solution in dichloromethane.<sup>[9,23]</sup> Successive experiments under the same experimental conditions showed that all formal reduction and oxidation potentials were reproducible within ±5 mV. Experimentally, the potentials were referenced against an Ag/Ag<sup>+</sup> reference electrode, but the results are presented referenced against ferrocene as an internal standard as required by IUPAC.<sup>[25]</sup> When dodecylferrocene was used as an internal standard, the experimentally measured potential was converted into *E*<sup>o'</sup> versus FcH/FcH<sup>+</sup> by the addition of -0.61 V.<sup>[37]</sup> Data were then manipulated on a Microsoft Excel worksheet to set the formal reduction potentials of the FcH/FcH<sup>+</sup> couple to *E*<sup>o'</sup> = 0.0 V. The cyclic voltammograms were taken after typical two scans and are considered to be steady-state cyclic voltammograms in which the event pattern does not differ from the initial sweep. To demonstrate that the compounds undergo no electrochemically induced polymerization reaction during the (spectro)-electrochemical measurements, **3a** was recorded for 20 cycles (Figure S6 in the Supporting Information).

**Single-Crystal X-ray Diffraction Analysis:** Data were collected with an Oxford Gemini S diffractometer using graphite-monochromatized Mo-*K*<sub>α</sub> radiation (λ = 0.71073 Å) (**2b**, **2c**, **3b**, **4b**, **5**, and **7b**) or Cu-*K*<sub>α</sub> radiation (λ = 1.54184 Å) (**3a**). The molecular structures were solved by direct methods using SHELXS-97<sup>[38]</sup> and refined by full-matrix least-squares procedures on *F*<sup>2</sup> using SHELXL-97.<sup>[39]</sup> All non-hydrogen atoms were refined anisotropically and a riding model was employed in the treatment of the hydrogen atom positions.

**1-Tosyl-1*H*-pyrrole (**1b**):** The title compound was synthesized according to literature methods.<sup>[12]</sup> Complementary to the physical data published there, we add the following crystal data: Suitable single crystals of **1b** were obtained by diffusion of methanol into a solution of **1b** in dichloromethane at ambient temperature. C<sub>11</sub>H<sub>11</sub>NO<sub>2</sub>S, *M*<sub>r</sub> = 221.27 g mol<sup>-1</sup>, 0.40 × 0.20 × 0.08 mm, orthorhombic, *Pna*2<sub>1</sub>, λ = 0.71073 Å, *a* = 19.8405(8) Å, *b* = 7.5428(3) Å, *c* = 28.2109(10) Å, *V* = 4221.8(3) Å<sup>3</sup>, *Z* = 16, ρ<sub>calcd.</sub> = 1.392 g cm<sup>-3</sup>, μ = 0.284 mm<sup>-1</sup>, *T* = 100(2) K, θ range = 2.98–25.50°, reflections collected 26192, independent 7587 (*R*<sub>int</sub> = 0.0647), *R*<sub>1</sub> = 0.0412, *wR*<sub>2</sub> = 0.0710 [*I* ≥ 2σ(*I*)].

**3,4-Dibromo-1-tosyl-1*H*-pyrrole (**2b**):** Molecule **2b** was synthesized according to the literature<sup>[12]</sup> with the following details: A solution of bromine (7.4 mL, 0.14 mol) in acetic acid (80 mL) was added over 30 min to a solution of **1b** (13.5 g, 0.06 mmol) in acetic acid (200 mL). The mixture was heated to reflux for 90 min. After all volatiles were removed under reduced pressure, a dark oil was obtained, which was filtered through silica using dichloromethane as the eluent. Afterwards, all volatiles were removed under vacuum and a dark solid was obtained. This was further purified by column chromatography (column size: 4 × 14 cm, silica) by using a *n*-hexane/toluene mixture with a ratio of 3:1 (v/v) as eluent (*R*<sub>f</sub> = 0.32). The analytical data are in agreement with the data given in the literature.<sup>[12]</sup> Yield 4.93 g (13.0 mmol, 21% based on **1b**). <sup>1</sup>H NMR

(CDCl<sub>3</sub>): δ = 2.44 (s, 3 H, CH<sub>3</sub>), 7.18 (s, 2 H, 2/5-H), 7.30–7.36 (m, 2 H, C<sub>6</sub>H<sub>4</sub>/*o*-CH<sub>3</sub>), 7.75–7.77 (m, 2 H, C<sub>6</sub>H<sub>4</sub>/*m*-CH<sub>3</sub>) ppm. <sup>13</sup>C{<sup>1</sup>H} NMR (CDCl<sub>3</sub>): δ = 21.7 (CH<sub>3</sub>), 105.3 (C-3/4), 120.0 (C-2/5), 127.2 (C<sub>6</sub>H<sub>4</sub>/*m*-CH<sub>3</sub>), 130.3 (C<sub>6</sub>H<sub>4</sub>/*o*-CH<sub>3</sub>), 134.9 (C-S), 146.0 (C-CH<sub>3</sub>) ppm.

**Crystal Data for 2b:** Suitable single crystals of **2b** were obtained by diffusion of methanol into a solution of **2b** in dichloromethane at ambient temperature. C<sub>11</sub>H<sub>9</sub>Br<sub>2</sub>NO<sub>2</sub>S, *M*<sub>r</sub> = 379.07 g mol<sup>-1</sup>, 0.45 × 0.35 × 0.35 mm, orthorhombic, *P*2<sub>1</sub>2<sub>1</sub>2<sub>1</sub>, λ = 0.71073 Å, *a* = 6.4496(3) Å, *b* = 13.3649(6) Å, *c* = 14.8341(6) Å, *V* = 1278.67(10) Å<sup>3</sup>, *Z* = 4, ρ<sub>calcd.</sub> = 1.969 g cm<sup>-3</sup>, μ = 6.491 mm<sup>-1</sup>, *T* = 100(2) K, θ range = 3.14–25.49°, reflections collected 5039, independent 2327 (*R*<sub>int</sub> = 0.0274), *R*<sub>1</sub> = 0.0322, *wR*<sub>2</sub> = 0.0738 [*I* ≥ 2σ(*I*)].

**3,4-Dibromo-1-(triisopropylsilyl)-1*H*-pyrrole (**2c**):** The title compound was prepared according to the literature<sup>[12]</sup> with the following details: THF was cooled to -80 °C and **1c** (2.89 g, 12.9 mmol) was added in a single portion. In the absence of light, NBS (4.60 g, 25.8 mmol) was added in a single portion, and the reaction mixture was stirred for 2 h at this temperature. After warming to ambient temperature, the solvent was removed under reduced pressure. Purification was realized by column chromatography (column size: 4 × 17 cm, silica) in the absence of light by using *n*-hexane as eluent to afford **2c** (*R*<sub>f</sub> = 0.46) as a colorless oil. The analytical data are in agreement with the literature.<sup>[12]</sup> Yield 3.97 g (10.4 mmol, 81% based on **1c**). <sup>1</sup>H NMR (CDCl<sub>3</sub>): δ = 1.09 (d, <sup>3</sup>*J*<sub>H,H</sub> = 7.5 Hz, 18 H, CH<sub>3</sub>), 1.40 (sept, <sup>3</sup>*J*<sub>H,H</sub> = 7.5 Hz, 3 H, CH), 6.72 (s, 2 H, 2/5-H) ppm. <sup>13</sup>C{<sup>1</sup>H} NMR (CDCl<sub>3</sub>): δ = 11.4 (CH), 17.6 (CH<sub>3</sub>), 101.0 (C-3/4), 123.7 (C-2/5) ppm.

**Crystal Data for 2c:** Suitable single crystals of **2c** were obtained by cooling a solution of **2c** in *n*-hexane to -30 °C. C<sub>13</sub>H<sub>23</sub>Br<sub>2</sub>NSi, *M*<sub>r</sub> = 381.23 g mol<sup>-1</sup>, 0.40 × 0.30 × 0.20 mm, triclinic, *P*1̄, λ = 0.71073 Å, *a* = 8.5693(8) Å, *b* = 9.5882(12) Å, *c* = 10.6196(14) Å, α = 78.462(11)°, β = 79.889(10)°, γ = 71.630(10)°, *V* = 805.39(16) Å<sup>3</sup>, *Z* = 2, ρ<sub>calcd.</sub> = 1.572 g cm<sup>-3</sup>, μ = 5.089 mm<sup>-1</sup>, *T* = 100(2) K, θ range = 3.01–25.07°, reflections collected 5480, independent 2830 (*R*<sub>int</sub> = 0.0266), *R*<sub>1</sub> = 0.0443, *wR*<sub>2</sub> = 0.1170 [*I* ≥ 2σ(*I*)].

**General Procedure: Synthesis of 3,4-diferrocenyl Pyrroles **3a**, **b** and **5**:** Ferrocene and KO*t*Bu (0.125 equiv.) were dissolved in THF (20 mL) and the respective solution was cooled to -80 °C. *tert*-Butyllithium (2 equiv., 1.6 M in *n*-pentane) was added dropwise with a syringe and the reaction solution was stirred for 1 h. Afterwards, [ZnCl<sub>2</sub>·2thf] (1 equiv.) was added in a single portion. The reaction mixture was stirred for an additional 30 min at 0 °C. Afterwards, 0.25 mol-% of [{Pd(CH<sub>2</sub>C(CH<sub>3</sub>)<sub>2</sub>P(*t*C<sub>4</sub>H<sub>9</sub>)<sub>2</sub>)(μ-Cl)}<sub>2</sub>] and bromopyrroles **2a**–**c** were added in a single portion, then stirring was continued overnight at 60–70 °C. The crude product was worked up by column chromatography with either silica or alumina by using different solvent mixtures (see below). All volatiles were removed under reduced pressure.

**3,4-Diferrocenyl-*N*-phenylpyrrole (**3a**):** Ferrocene (0.278 g, 1.49 mmol), KO*t*Bu (0.125 equiv., 22.6 mg, 0.2 mmol), *tert*-butyllithium (2 equiv., 1.86 mL, 2.98 mmol), [ZnCl<sub>2</sub>·2thf] (1.0 equiv., 0.42 mg, 1.49 mmol), **2a** (1/3 equiv., 0.15 g, 0.5 mmol), and [{Pd(CH<sub>2</sub>C(CH<sub>3</sub>)<sub>2</sub>P(*t*C<sub>4</sub>H<sub>9</sub>)<sub>2</sub>)(μ-Cl)}<sub>2</sub>] (0.25 mol-%, 0.85 mg, 0.001 mmol) were used in the reaction. As eluent for column chromatography (column size: 1.5 × 10 cm; alumina pretreated with triethylamine) an *n*-hexane/diethyl ether mixture (10:1 v/v) was used. Compound **3a** was obtained as a pale orange solid, yield 0.111 g (0.217 mmol, 87% on the basis of **2a**), m.p. 183 °C. <sup>1</sup>H NMR (CDCl<sub>3</sub>): δ = 4.09 (s, 10 H, C<sub>5</sub>H<sub>5</sub>), 4.18 (pt, *J*<sub>H,H</sub> = 1.8 Hz, 4 H, C<sub>5</sub>H<sub>4</sub>), 4.33 (pt, *J*<sub>H,H</sub> = 1.8 Hz, 4 H, C<sub>5</sub>H<sub>4</sub>), 7.18 (s, 2 H, 2/5-H), 7.19 (m, 1 H, *p*-C<sub>6</sub>H<sub>5</sub>), 7.47 (m, 4 H, C<sub>6</sub>H<sub>5</sub>) ppm. <sup>13</sup>C{<sup>1</sup>H}

NMR (CDCl<sub>3</sub>):  $\delta$  = 67.48 (C<sub>5</sub>H<sub>4</sub>), 69.21 (C<sub>5</sub>H<sub>4</sub>), 69.34 (C<sub>5</sub>H<sub>5</sub>), 81.83 (C<sub>7</sub>-C<sub>5</sub>H<sub>4</sub>), 118.24 (C-2/5), 120.13 (C<sub>6</sub>H<sub>5</sub>), 122.80 (C-3/4), 125.62 (C<sub>6</sub>H<sub>5</sub>), 129.80 (C<sub>6</sub>H<sub>5</sub>), 140.59 (C<sub>7</sub>-C<sub>6</sub>H<sub>5</sub>) ppm. IR (KBr):  $\tilde{\nu}$  = 757 (s,  $\gamma_{\text{o.o.p.}}$  = C-H), 1065 (m,  $\nu_{\text{C-N}}$ ), 1498 (s,  $\nu_{\text{C=C}}$ ), 1595 (m,  $\nu_{\text{C=C}}$ ), 3091 (w,  $\nu_{\text{C-H}}$ ) cm<sup>-1</sup>. HRMS (ESI-TOF): calcd. for C<sub>30</sub>H<sub>25</sub>NFe<sub>2</sub> 511.0681; found 511.0691 [M]<sup>+</sup>. C<sub>30</sub>H<sub>25</sub>Fe<sub>2</sub>N (511.22 g mol<sup>-1</sup>): calcd. C 70.48, H 4.93, N 2.74; found C 70.54, H 4.91, N 2.71.

**Crystal Data for 3a:** Single crystals of **3a** were obtained by diffusion of toluene into a solution of **3a** in dichloromethane at 25 °C. C<sub>30</sub>H<sub>25</sub>Fe<sub>2</sub>N,  $M_r$  = 511.21 g mol<sup>-1</sup>, 0.28 × 0.12 × 0.03 mm, monoclinic,  $P2_1/c$ ,  $\lambda$  = 1.54184 Å,  $a$  = 26.7104(16) Å,  $b$  = 6.1920(4) Å,  $c$  = 27.9684(14) Å,  $\beta$  = 108.587(6)°,  $V$  = 4384.4(4) Å<sup>3</sup>,  $Z$  = 8,  $\rho_{\text{calcd.}}$  = 1.549 g cm<sup>-3</sup>,  $\mu$  = 10.745 mm<sup>-1</sup>,  $T$  = 100 K,  $\theta$  range = 3.23–64.08°, reflections collected 13430, independent 7109 ( $R_{\text{int}}$  = 0.0419),  $R_1$  = 0.0513,  $wR_2$  = 0.1251 [ $I \geq 2\sigma(I)$ ].

**3,4-Diferrocenyl-1-tosyl-1H-pyrrole (3b):** Ferrocene (2.496 g, 13.2 mmol), KO<sup>t</sup>Bu (0.125 equiv., 59 mg, 0.53 mmol), *tert*-butyllithium (2 equiv., 16.5 mL, 26.4 mmol), [ZnCl<sub>2</sub>·2thf] (1.0 equiv., 3.7 g, 13.2 mmol), **2b** (1/3 equiv., 2.00 g, 5.28 mmol), and [Pd(CH<sub>2</sub>C(CH<sub>3</sub>)<sub>2</sub>P(*t*C<sub>4</sub>H<sub>9</sub>)<sub>2</sub>)( $\mu$ -Cl)]<sub>2</sub> (1 mol-%, 36 mg, 0.05 mmol) were used in the reaction. As eluent for column chromatography (column size: 4 × 16 cm, alumina) an *n*-hexane/toluene mixture (4:1 v/v) was used. Compound **3b** was obtained as an orange solid, yield 0.530 g (0.90 mmol, 17% on the basis of **2b**), m.p. 214 °C. <sup>1</sup>H NMR (CDCl<sub>3</sub>):  $\delta$  = 2.42 (s, 3 H, CH<sub>3</sub>), 4.07 (s, 10 H, C<sub>5</sub>H<sub>5</sub>), 4.23 (m, 4 H, C<sub>5</sub>H<sub>4</sub>), 4.33 (m, 4 H, C<sub>5</sub>H<sub>4</sub>), 7.12 (s, 2 H, 2/5-H), 7.33–7.35 (m, 2 H, C<sub>6</sub>H<sub>4</sub>/*o*-CH<sub>3</sub>), 7.81–7.82 (m, 2 H, C<sub>6</sub>H<sub>4</sub>/*m*-CH<sub>3</sub>) ppm. <sup>13</sup>C{<sup>1</sup>H} NMR (CDCl<sub>3</sub>):  $\delta$  = 21.6 (CH<sub>3</sub>), 67.9 (C<sub>5</sub>H<sub>4</sub>), 69.3 (C<sub>5</sub>H<sub>4</sub>), 69.5 (C<sub>5</sub>H<sub>5</sub>), 79.6 (C<sub>7</sub>-C<sub>5</sub>H<sub>4</sub>), 118.8 (C-2/5), 126.6 (C-3/4), 126.8 (C<sub>6</sub>H<sub>4</sub>/*m*-CH<sub>3</sub>), 130.0 (C<sub>6</sub>H<sub>4</sub>/*o*-CH<sub>3</sub>), 136.1 (C-S), 145.0 (C-CH<sub>3</sub>) ppm. IR (KBr):  $\tilde{\nu}$  = 3091 (w,  $\nu_{\text{C-H}}$ ), 2921 (w,  $\nu_{\text{CH}_3}$ ), 2848 (w,  $\nu_{\text{CH}_3}$ ), 1596 (w), 1492 (w), 1441 (w), 1411 (w), 1370 (s,  $\nu_{\text{SO}_2}$ ), 1300 (m), 1257 (w), 1187 (w) 1172 (s,  $\nu_{\text{SO}_2}$ ), 1124 (m), 1106 (w), 1090 (w), 1070 (m), 1060 (m), 1001 (w), 968 (w), 889 (w), 816 (m,  $\gamma_{\text{Fc-H}}$ ), 806 (m), 781 (m), 702 (w), 673 (m), 610 (m), 587 (m), 539 (m) cm<sup>-1</sup>. UV/Vis (CHCl<sub>3</sub>):  $\lambda$  (log  $\epsilon$ ) = 230 (4.61), 336 (3.19), 446 (2.65) nm. HRMS (ESI-TOF): calcd. for C<sub>31</sub>H<sub>28</sub>Fe<sub>2</sub>NO<sub>2</sub>S 589.0427; found 590.0466 [M + H]<sup>+</sup>. C<sub>31</sub>H<sub>27</sub>Fe<sub>2</sub>NO<sub>2</sub>S (589.31 g mol<sup>-1</sup>): calcd. C 63.18, H 4.62, N 2.38; found C 63.23, H 4.71, N 2.40.

**Crystal Data for 3b:** Suitable single crystals of **3b** were obtained by diffusion of methanol into a solution of **3b** in dichloromethane at ambient temperature. C<sub>31</sub>H<sub>27</sub>Fe<sub>2</sub>NO<sub>2</sub>S,  $M_r$  = 589.30 g mol<sup>-1</sup>, 0.40 × 0.40 × 0.40 mm, triclinic,  $P\bar{1}$ ,  $\lambda$  = 0.71073 Å,  $a$  = 10.4805(9) Å,  $b$  = 10.7282(11) Å,  $c$  = 12.1127(16) Å,  $\alpha$  = 103.238(10)°,  $\beta$  = 92.251(9)°,  $\gamma$  = 108.304(9)°,  $V$  = 1249.5(2) Å<sup>3</sup>,  $Z$  = 2,  $\rho_{\text{calcd.}}$  = 1.566 g cm<sup>-3</sup>,  $\mu$  = 1.276 mm<sup>-1</sup>,  $T$  = 100(2) K,  $\theta$  range = 3.02–25.50°, reflections collected 8015, independent 4620 ( $R_{\text{int}}$  = 0.0279),  $R_1$  = 0.0345,  $wR_2$  = 0.0800 [ $I \geq 2\sigma(I)$ ].

**2,3-Diferrocenyl-N-phenylpyrrole (5):** Ferrocene (1.7016 g, 9.1 mmol), KO<sup>t</sup>Bu (0.125 equiv., 127 mg, 1.14 mmol), *tert*-butyllithium (2 equiv., 6.0 mL, 9.6 mmol), [ZnCl<sub>2</sub>·2thf] (1.0 equiv., 2.55 g, 9.1 mmol), **2b** (1/3 equiv., 1.000 g, 3.05 mmol), and [Pd(CH<sub>2</sub>C(CH<sub>3</sub>)<sub>2</sub>P(*t*C<sub>4</sub>H<sub>9</sub>)<sub>2</sub>)( $\mu$ -Cl)]<sub>2</sub> (68 mg, 0.1 mmol) were used in the reaction. Compound **5** was obtained by crystallization from a solution of **5** in chloroform, whereby a few single crystals formed. HRMS (ESI-TOF): calcd. for C<sub>33</sub>H<sub>41</sub>Fe<sub>2</sub>NSi 591.1703; found 591.1654 [M]<sup>+</sup>.

**Crystal Data for 5:** Suitable single crystals of **5** were obtained by slow evaporation of a solution of **5** in chloroform at ambient temperature. C<sub>33</sub>H<sub>41</sub>Fe<sub>2</sub>NSi,  $M_r$  = 591.46 g mol<sup>-1</sup>,

0.30 × 0.20 × 0.20 mm, monoclinic,  $P2_1/n$ ,  $\lambda$  = 0.71073 Å,  $a$  = 22.5202(8) Å,  $b$  = 10.9924(3) Å,  $c$  = 34.3380(12) Å,  $\beta$  = 94.221(3)°,  $V$  = 8477.3(5) Å<sup>3</sup>,  $Z$  = 12,  $\rho_{\text{calcd.}}$  = 1.390 g cm<sup>-3</sup>,  $\mu$  = 1.092 mm<sup>-1</sup>,  $T$  = 100(3) K,  $\theta$  range = 3.10–25.25°, reflections collected 41621, independent 15292 ( $R_{\text{int}}$  = 0.0477),  $R_1$  = 0.0591,  $wR_2$  = 0.1530 [ $I \geq 2\sigma(I)$ ].

**General Procedure for the Synthesis of 4a,b and 7a,b:** For the Sonogashira C–C cross-coupling reactions, [CuI] (6 mol-%) and [PdCl<sub>2</sub>(PPh<sub>3</sub>)<sub>2</sub>] (1 mol-%) were dissolved in NH<sub>4</sub>Pr<sub>2</sub> (60 mL) and the reaction mixture was stirred for 10 min. The orange solution was treated with 2,5-Br<sub>2</sub>-c-C<sub>4</sub>H<sub>2</sub>NR (1 equiv.; R = Ph (**2a**), SO<sub>2</sub>-4-MeC<sub>6</sub>H<sub>4</sub> (**2b**)), ethynylferrocene (2.1 equiv.), and triphenylphosphane (6 mol-%) and was heated to reflux overnight. The reaction mixture was cooled to ambient temperature and all volatiles were removed in an oil-pump vacuum. The residue was washed with diethyl ether, and the solution was filtered through a pad of Celite to remove the ammonium salt. The Celite was washed with diethyl ether until the solvent was colorless. The orange filtrate was concentrated and purified by column chromatography using either silica or alumina and different solvent mixtures (see below). All volatiles were removed under reduced pressure.

**Data for 3,4-Bis(ferrocenylethynyl)-N-phenylpyrrole (4a) and 3-Bromo-4-ferrocenylethynyl-N-phenylpyrrole (7a):** Compound **2a** (0.352 g, 1.17 mmol), [CuI] (14 mg, 0.07 mmol), [PdCl<sub>2</sub>(PPh<sub>3</sub>)<sub>2</sub>] (8.4 mg, 0.012 mmol), PPh<sub>3</sub> (18.4 mg, 0.07 mmol), and FcC≡CH (2.1 equiv.; 517 mg, 2.46 mol) were used in the reaction. As eluent for column chromatography (column size 4 × 14 cm, alumina) an *n*-hexane/diethyl ether mixture (10:1 v/v) was used to elute **7a**, whereas with a ratio of 2:1 (v/v), compound **4a** could be eluted as an orange band. After removal of all volatiles under vacuum, compound **4a** could be obtained as orange solid, whereas **7a** was isolated as an red oil.

**Compound 4a:** Yield 0.177 g (0.316 mmol, 27% on the basis of **2a**), m.p. 145 °C. <sup>1</sup>H NMR (CDCl<sub>3</sub>):  $\delta$  = 4.09 (s, 10 H, C<sub>5</sub>H<sub>5</sub>), 4.18 (pt,  $J_{\text{H,H}}$  = 1.8 Hz, 4 H, C<sub>5</sub>H<sub>4</sub>), 4.33 (pt,  $J_{\text{H,H}}$  = 1.8 Hz, 4 H, C<sub>5</sub>H<sub>4</sub>), 7.18 (s, 2 H, 2/5-H), 7.19 (m, 1 H, *p*-C<sub>6</sub>H<sub>5</sub>), 7.47 (m, 4 H, C<sub>6</sub>H<sub>5</sub>) ppm. <sup>13</sup>C{<sup>1</sup>H} NMR (CDCl<sub>3</sub>):  $\delta$  = 66.09 (C≡C), 68.76 (C<sub>5</sub>H<sub>4</sub>), 70.26 (C<sub>5</sub>H<sub>5</sub>), 71.60 (C<sub>5</sub>H<sub>4</sub>), 78.74 (C<sub>7</sub>-C<sub>5</sub>H<sub>4</sub>), 89.83 (C≡C), 110.50 (C-3/4), 120.71 (C<sub>6</sub>H<sub>5</sub>), 122.55 (C-2/5), 126.75 (*p*-C<sub>6</sub>H<sub>5</sub>), 129.95 (C<sub>6</sub>H<sub>5</sub>), 139.75 (C<sub>7</sub>-C<sub>6</sub>H<sub>5</sub>) ppm. IR (KBr):  $\tilde{\nu}$  = 758 (s,  $\gamma_{\text{o.o.p.}}$  = C-H), 1062 (m,  $\nu_{\text{C-N}}$ ), 1504 (s,  $\nu_{\text{C=C}}$ ), 1598 (m,  $\nu_{\text{C=C}}$ ), 2208 (w,  $\nu_{\text{C=C}}$ ), 3091 (w,  $\nu_{\text{C-H}}$ ) cm<sup>-1</sup>. HRMS (ESI-TOF): calcd. for C<sub>34</sub>H<sub>25</sub>NFe<sub>2</sub> 559.0681; found 559.0697 [M]<sup>+</sup>.

**Compound 7a:** Yield 0.195 g (0.453 mmol, 39% on the basis of **2a**). <sup>1</sup>H NMR (CDCl<sub>3</sub>):  $\delta$  = 4.23 (pt,  $J_{\text{H,H}}$  = 1.9 Hz, 2 H, C<sub>5</sub>H<sub>4</sub>), 4.28 (s, 5 H, C<sub>5</sub>H<sub>5</sub>), 4.52 (pt,  $J_{\text{H,H}}$  = 1.9 Hz, 2 H, C<sub>5</sub>H<sub>4</sub>), 7.07 (d,  $^4J_{\text{H}_2\text{H}_5}$  = 2.5 Hz, 1 H, 2-H), 7.24 (d,  $^4J_{\text{H}_5\text{H}_2}$  = 2.5 Hz, 1 H, 5-H), 7.30–7.35 (m, 3 H, C<sub>6</sub>H<sub>5</sub>), 7.45 (m, 2 H, C<sub>6</sub>H<sub>5</sub>) ppm. <sup>13</sup>C{<sup>1</sup>H} NMR (CDCl<sub>3</sub>):  $\delta$  = 65.62 (C≡C), 68.83 (C<sub>5</sub>H<sub>4</sub>), 70.21 (C<sub>5</sub>H<sub>5</sub>), 71.66 (C<sub>5</sub>H<sub>4</sub>), 77.64 (C<sub>7</sub>-C<sub>5</sub>H<sub>4</sub>), 90.44 (C≡C), 101.96 (C-4), 109.62 (C-3), 119.62 (C-5), 126.83 (C-2), 120.57 (C<sub>6</sub>H<sub>5</sub>), 122.65 (*p*-C<sub>6</sub>H<sub>5</sub>), 129.94 (C<sub>6</sub>H<sub>5</sub>), 139.68 (C<sub>7</sub>-C<sub>6</sub>H<sub>5</sub>) ppm. IR (NaCl):  $\tilde{\nu}$  = 758 (s,  $\gamma_{\text{o.o.p.}}$  = C-H), 1023 (m,  $\nu_{\text{C-N}}$ ), 1495 (s,  $\nu_{\text{C=C}}$ ), 1598 (m,  $\nu_{\text{C=C}}$ ), 2240 (w,  $\nu_{\text{C=C}}$ ), 3097 (w,  $\nu_{\text{C-H}}$ ) cm<sup>-1</sup>. HRMS (ESI-TOF): calcd. for C<sub>22</sub>H<sub>16</sub>NFeBr 428.9812; found 428.9798 [M]<sup>+</sup>.

**3,4-Bis(ferrocenylethynyl)-1-tosyl-1H-pyrrole (4b) and 3-Bromo-4-ferrocenylethynyl-1-tosyl-1H-pyrrole (7b):** 3,4-Dibromo-*N*-tosylpyrrole (**2b**) (860 g, 2.27 mmol), [CuI] (27 mg, 0.14 mmol), [PdCl<sub>2</sub>(PPh<sub>3</sub>)<sub>2</sub>] (16.1 mg, 0.023 mmol), PPh<sub>3</sub> (35.7 mg, 0.14 mmol), and FcC≡CH (2.1 equiv., 1.00 g, 4.77 mol) were used in the reaction. Purification was realized by column chromatography (column size 4 × 18 cm, alumina) by using a 1:1 (v/v) toluene/*n*-hexane mix-

ture as eluent to obtain first **7b** and second **4b**. After removal of all volatile materials, compounds **7b** ( $R_f = 0.67$ ) and **4b** ( $R_f = 0.52$ ) were isolated as orange solids.

**Compound 4b:** Yield 0.254 g (0.40 mmol, 18% based on **2b**), m.p. 183 °C.  $^1\text{H NMR}$  ( $\text{CDCl}_3$ ):  $\delta = 2.43$  (s, 3 H,  $\text{CH}_3$ ), 4.21 (pt,  $J_{\text{H,H}} = 1.8$  Hz, 4 H,  $\text{C}_5\text{H}_4$ ), 4.23 (s, 10 H,  $\text{C}_5\text{H}_5$ ), 4.48 (pt,  $J_{\text{H,H}} = 1.8$  Hz, 4 H,  $\text{C}_5\text{H}_4$ ), 7.27 (s, 2 H, 2/5-H), 7.32–7.34 (m, 2 H,  $\text{C}_6\text{H}_4/o\text{-CH}_3$ ), 7.78–7.80 (m, 2 H,  $\text{C}_6\text{H}_4/m\text{-CH}_3$ ) ppm.  $^{13}\text{C}\{^1\text{H}\}$  NMR ( $\text{CDCl}_3$ ):  $\delta = 21.7$  ( $\text{CH}_3$ ), 64.8 ( $\text{C}_f\text{-C}_5\text{H}_4$ ), 69.0 ( $\text{C}_5\text{H}_4$ ), 70.1 ( $\text{C}_5\text{H}_5$ ), 71.5 ( $\text{C}_5\text{H}_4$ ), 76.9 ( $\text{C}\equiv\text{C}$ ), 91.4 ( $\text{C}\equiv\text{C}$ ), 113.2 (C-3/4), 122.6 (C-2/5), 127.2 ( $\text{C}_6\text{H}_4/m\text{-CH}_3$ ), 130.2 ( $\text{C}_6\text{H}_4/m\text{-CH}_3$ ), 135.2 (C-S), 145.7 (C- $\text{CH}_3$ ) ppm. IR (NaCl):  $\tilde{\nu} = 3140$  (w,  $\nu_{\text{C-H}}$ ), 3094 (w,  $\nu_{\text{C-H}}$ ), 2964 (w,  $\nu_{\text{CCH}_3}$ ), 2923 (w), 2853 (w,  $\nu_{\text{CCH}_3}$ ), 2215 (m,  $\nu_{\text{C=C}}$ ), 1595 (w), 1448 (w), 1411 (w), 1378 (m,  $\nu_{\text{SO}_2}$ ), 1319 (m), 1286 (w), 1213 (w), 1190 (m), 1173 (s,  $\nu_{\text{SO}_2}$ ), 1121 (w), 1105 (w), 1091 (m), 1065 (s), 1027 (m), 1002 (m), 966 (w), 926 (w), 814 (s,  $\gamma_{\text{C-H}}$ ), 761 (w), 702 (m), 671 (m), 585 (s), 534 (m)  $\text{cm}^{-1}$ . UV/Vis ( $\text{CHCl}_3$ ):  $\lambda = 231$ , 279, 445 nm. HRMS (ESI-TOF): calcd. for  $\text{C}_{35}\text{H}_{27}\text{Fe}_2\text{NO}_2\text{S}$  637.0457; found 637.0477 [ $\text{M}$ ] $^+$ .

**Crystal Data for 4b:** Suitable single crystals of **4b** were obtained by the diffusion of methanol into a solution of **4b** in dichloromethane at ambient temperature.  $\text{C}_{35}\text{H}_{27}\text{Fe}_2\text{NO}_2\text{S}$ ,  $M_r = 637.34$   $\text{g mol}^{-1}$ ,  $0.40 \times 0.35 \times 0.35$  mm, triclinic,  $P\bar{1}$ ,  $\lambda = 0.71073$  Å,  $a = 9.3833(5)$  Å,  $b = 10.7499(8)$  Å,  $c = 14.1386(7)$  Å,  $\alpha = 78.728(5)^\circ$ ,  $\beta = 84.988(4)^\circ$ ,  $\gamma = 79.113(5)^\circ$ ,  $V = 1371.56(14)$  Å $^3$ ,  $Z = 2$ ,  $\rho_{\text{calcd.}} = 1.543$   $\text{g cm}^{-3}$ ,  $\mu = 1.169$   $\text{mm}^{-1}$ ,  $T = 100(2)$  K,  $\theta$  range = 2.94–25.50°, reflections collected 8951, independent 5061 ( $R_{\text{int}} = 0.0200$ ),  $R_1 = 0.0291$ ,  $wR_2 = 0.0707$  [ $I \geq 2\sigma(I)$ ].

**Compound 7b:** Yield 0.300 g (0.59 mmol, 26% on the basis of **2b**), m.p. 160 °C.  $^1\text{H NMR}$  ( $\text{CDCl}_3$ ):  $\delta = 2.43$  (s, 3 H,  $\text{CH}_3$ ), 4.23 (pt,  $J_{\text{H,H}} = 1.8$  Hz, 2 H,  $\text{C}_5\text{H}_4$ ), 4.24 (s, 5 H,  $\text{C}_5\text{H}_5$ ), 4.48 (pt,  $J_{\text{H,H}} = 1.8$  Hz, 2 H,  $\text{C}_5\text{H}_4$ ), 7.16 (d,  $J_{\text{H,H}} = 2.5$  Hz, 1 H, 5-H), 7.28 (d,  $J_{\text{H,H}} = 2.5$  Hz, 1 H, 2-H), 7.32–7.34 (m, 2 H,  $\text{C}_6\text{H}_4$ ), 7.76–7.78 (m, 2 H,  $\text{C}_6\text{H}_4$ ) ppm.  $^{13}\text{C}\{^1\text{H}\}$  NMR ( $\text{CDCl}_3$ ):  $\delta = 21.7$  ( $\text{CH}_3$ ), 64.4 (C- $\text{C}_5\text{H}_4$ ), 68.9 ( $\text{C}_5\text{H}_4$ ), 70.1 ( $\text{C}_5\text{H}_5$ ), 71.6 ( $\text{C}_5\text{H}_4$ ), 75.8 ( $\text{C}\equiv\text{C}$ ), 92.3 ( $\text{C}\equiv\text{C}$ ), 105.3 (C-3), 112.9 (C-4), 119.7 (C-5), 122.8 (C-2), 127.2 ( $\text{C}_6\text{H}_4$ ), 130.3 ( $\text{C}_6\text{H}_4$ ), 135.1 (C-S), 145.8 (C- $\text{CH}_3$ ) ppm. IR (NaCl):  $\tilde{\nu} = 3138$  (m,  $\nu_{\text{C-H}}$ ), 3095 (w,  $\nu_{\text{C-H}}$ ), 2955 (w,  $\nu_{\text{CCH}_3}$ ), 2923 (w), 2854 (w,  $\nu_{\text{CCH}_3}$ ), 2223 (m,  $\nu_{\text{C=C}}$ ), 1595 (m), 1555 (w), 1494 (w), 1448 (w), 1379 (s), 1309 (s,  $\nu_{\text{SO}_2}$ ), 1217 (s), 1189 (s), 1174 (s,  $\nu_{\text{SO}_2}$ ), 1090 (w), 1074 (s), 1047 (m), 1020 (m), 1002 (w), 960 (m), 916 (w), 813 [ $m$  ( $\gamma = \text{C-H}$ )], 793 (m), 718 (w), 701 (w), 671 (s), 596 (s), 585 (m), 536 (m)  $\text{cm}^{-1}$ . UV/Vis ( $\text{CH}_2\text{Cl}_2$ ):  $\lambda = 230$ , 265, 445 nm. HRMS (ESI-TOF): calcd. for  $\text{C}_{23}\text{H}_{18}\text{BrFeNO}_2\text{S}$  506.9587; found 506.9610 [ $\text{M}$ ] $^+$ .

**Crystal Data for 7b:** Suitable single crystals of **7b** were obtained by the diffusion of methanol into a solution of **7b** in dichloromethane at ambient temperature.  $\text{C}_{23}\text{H}_{18}\text{BrFeNO}_2\text{S}$ ,  $M_r = 508.20$   $\text{g mol}^{-1}$ ,  $0.50 \times 0.40 \times 0.35$  mm, triclinic,  $P\bar{1}$ ,  $\lambda = 0.71073$  Å,  $a = 9.6481(12)$  Å,  $b = 11.0576(12)$  Å,  $c = 11.3090(14)$  Å,  $\alpha = 76.213(10)^\circ$ ,  $\beta = 65.546(13)^\circ$ ,  $\gamma = 69.762(11)^\circ$ ,  $V = 1024.1(2)$  Å $^3$ ,  $Z = 2$ ,  $\rho_{\text{calcd.}} = 1.648$   $\text{g cm}^{-3}$ ,  $\mu = 2.809$   $\text{mm}^{-1}$ ,  $T = 100(2)$  K,  $\theta$  range = 3.52–25.49°, reflections collected 6964, independent 3799 ( $R_{\text{int}} = 0.0244$ ),  $R_1 = 0.0277$ ,  $wR_2 = 0.0678$  [ $I \geq 2\sigma(I)$ ].

CCDC-967395 (for **2c**), -967396 (for **5**), -967397 (for **1b**), -967398 (for **2b**), -967399 (for **3b**), -967400 (for **7b**), -967401 (for **4b**), and -967402 (for **3a**) contain the supplementary crystallographic data for this paper. These data can be obtained free of charge from The Cambridge Crystallographic Data Centre via www.ccdc.cam.ac.uk/data\_request/cif.

**Supporting Information** (see footnote on the first page of this article): Figures and CIF files giving additional experimental and crystallographic data.

## Acknowledgments

The authors are grateful to the Fonds der Chemischen Industrie (FCI) for financial support. M. K. thanks the Fonds der Chemischen Industrie for a fellowship. Dipl.-Chem. Dieter Schaarschmidt is thanked for many fruitful discussions.

- [1] M. Iyoda, T. Kondo, T. Okabe, H. Matsuyama, S. Sasaki, Y. A. Kuwatani, *Chem. Lett.* **1997**, *26*, 35–36.
- [2] A. Hildebrandt, D. Schaarschmidt, R. Claus, H. Lang, *Inorg. Chem.* **2011**, *50*, 10623–10632.
- [3] a) D. Miesel, A. Hildebrandt, M. Korb, P. J. Low, H. Lang, *Organometallics* **2013**, *32*, 2993–3002; b) P. V. Solntsev, S. V. Dudkin, J. R. Sabin, V. N. Nemykin, *Organometallics* **2011**, *30*, 3037–3046; c) A. Hildebrandt, S. W. Lechrich, D. Schaarschmidt, R. Jaeschke, K. Schreiter, S. Spange, H. Lang, *Eur. J. Inorg. Chem.* **2012**, 1114–1121.
- [4] K. Kaleta, A. Hildebrandt, F. Strehler, P. Arndt, H. Jiao, A. Spannenberg, H. Lang, U. Rosenthal, *Angew. Chem.* **2011**, *123*, 11444–11448; *Angew. Chem. Int. Ed.* **2011**, *50*, 11248–11252.
- [5] K. Kaleta, F. Strehler, A. Hildebrandt, T. Beweries, P. Arndt, T. Ruffer, A. Spannenberg, H. Lang, U. Rosenthal, *Chem. Eur. J.* **2012**, *18*, 12672–12680.
- [6] A. Hildebrandt, H. Lang, *Organometallics* **2013**, *32*, 5640–5653.
- [7] a) S. C. Jones, S. Barlow, D. O'Hare, *Chem. Eur. J.* **2005**, *11*, 4473–4481; b) S. Barlow, D. O'Hare, *Chem. Rev.* **1997**, *97*, 637–670; I. M. Bruce, *Coord. Chem. Rev.* **1997**, *166*, 91–119; c) M. Ratner, J. Jortner, *Molecular Electronics*, Blackwell Science, Malden, MA, **1997**; d) M. K. Tour, *Acc. Chem. Res.* **2000**, *33*, 791–804; e) P. C. Collier, W. E. Wong, M. Belohradsky, M. F. Raymo, F. J. Stoddart, J. P. Kuekes, S. R. Williams, R. J. Heath, *Science* **1999**, *285*, 391–394; f) R. L. Carroll, Ch. B. Gorman, *Angew. Chem.* **2002**, *114*, 4556–4579; *Angew. Chem. Int. Ed.* **2002**, *41*, 4378–4400; g) N. Robertson, C. A. McGowan, *Chem. Soc. Rev.* **2003**, *32*, 96–103.
- [8] A. Hildebrandt, T. Ruffer, E. Erasmus, J. C. Swarts, H. Lang, *Organometallics* **2010**, *29*, 4900–4905.
- [9] A. Hildebrandt, D. Schaarschmidt, H. Lang, *Organometallics* **2011**, *30*, 556–563.
- [10] A. Hildebrandt, H. Lang, *Dalton Trans.* **2011**, *40*, 11831–11837.
- [11] J. M. Speck, R. Claus, A. Hildebrandt, T. Ruffer, E. Erasmus, L. van As, J. C. Swarts, H. Lang, *Organometallics* **2012**, *31*, 6373–6380.
- [12] a) B. L. Bray, P. H. Mathies, R. Naef, D. R. Solas, T. T. Tidwell, *J. Org. Chem.* **1990**, *55*, 6317–6328; b) C. Zonta, F. Fabris, O. De Lucchi, *Org. Lett.* **2005**, *7*, 1003–1006.
- [13] D.-S. Choi, S. Huang, M. Huang, T. S. Barnard, R. D. Adams, J. M. Seminario, J. M. Tour, *J. Org. Chem.* **1998**, *63*, 2646–2655.
- [14] P. W. Shum, A. P. Koxikowski, *Tetrahedron Lett.* **1990**, *31*, 6785–6788.
- [15] a) S. Takahashi, Y. Kuroyama, K. Sonogashira, N. Hagihara, *Synthesis* **1980**, 627–629; b) K. Sonogashira, in: *Metal-Catalyzed Cross-Coupling Reactions* (Eds.: F. Diederich, P. J. Stang), Wiley-VCH, Weinheim, Germany, **1998**; c) K. Kobayashi, N. Kobayashi, *J. Org. Chem.* **2004**, *69*, 2487–2497.
- [16] a) T. Fukuda, E. Sudo, K. Shimokawa, M. Iwao, *Tetrahedron* **2008**, *64*, 328–338; b) V. Stockmann, K. L. Eriksen, A. Fiksdahl, *Tetrahedron* **2008**, *64*, 11180–11184; c) A. Fürstner, H. Krause, O. R. Thiel, *Tetrahedron* **2002**, *58*, 6373–6380; d) C. Zonta, F. Fabris, O. De Lucchi, *Org. Lett.* **2005**, *7*, 1003–6380.
- [17] a) S. Gronowitz, *Chem. Heterocycl. Compd.* **1994**, *30*, 1252–1283; b) S. Gronowitz, B. Holm, *Acta Chem. Scand.* **1976**, *30*,

- 505–511; c) N. Proust, M. F. Chellat, J. P. Stambuli, *Synthesis* **2011**, 3083–3088; d) M. Schnürch, M. Spina, A. F. Khan, M. D. Mihovilovic, P. Stanetty, *Chem. Soc. Rev.* **2007**, *36*, 1046–1057; e) X. Wu, N.-A. Chen, L. Zhu, R. D. Rieke, *Tetrahedron Lett.* **1994**, *35*, 3673–3674; f) S. Gronowitz, B. Holm, *Acta Chem. Scand.* **1976**, *30*, 505–511.
- [18] H. Günther, *Angew. Chem.* **1972**, *84*, 907–920; *Angew. Chem. Int. Ed. Engl.* **1972**, *11*, 861–874.
- [19] H. Günzler, H. Böck, *IR-Spektroskopie*, Verlag Chemie, Weinheim, Germany, 2nd revised ed., **1983**.
- [20] The  $\tau$  parameter can be calculated as follows:  $\tau = 1 + \left\{ \frac{(d_{C-C} - d_{C=C})}{d_{C=C}} - 1 \right\} / \left\{ 1 - \frac{(d_{C-C}^0 - d_{C=C}^0)}{d_{C=C}^0} \right\}$ ;  $d_{C-C}^0 = 1.54 \text{ \AA}$ ;  $d_{C=C}^0 = 1.34 \text{ \AA}$ .
- [21] U. Pfaff, A. Hildebrandt, D. Schaarschmidt, T. Ruffer, P. J. Low, H. Lang, *Organometallics* **2013**, *32*, 6106–6117.
- [22] For information concerning the use of  $[NnBu_4][B(C_6F_5)_4]$  as supporting electrolyte, see: a) R. J. LeSuer, C. Buttolph, W. E. Geiger, *Anal. Chem.* **2004**, *76*, 6395–401; b) F. Barrière, W. E. Geiger, *J. Am. Chem. Soc.* **2006**, *128*, 3980–3989.
- [23] For examples of the application of  $[NnBu_4][B(C_6F_5)_4]$  as supporting electrolyte within electrochemical measurements, see: a) H. J. Gericke, N. I. Barnard, E. Erasmus, J. C. Swarts, M. J. Cook, M. a. S. Aquino, *Inorg. Chim. Acta* **2010**, *363*, 2222–2232; b) E. Fourie, J. C. Swarts, D. Lorcy, N. Bellec, *Inorg. Chem.* **2010**, *49*, 952–959; c) J. C. Swarts, A. Nafady, J. H. Roubush, S. Trupia, W. E. Geiger, *Inorg. Chem.* **2009**, *48*, 2156–2165; d) D. Chong, J. Slote, W. E. Geiger, *J. Electroanal. Chem.* **2009**, *630*, 28–34; e) V. N. Nemykin, G. T. Rohde, C. D. Barrett, R. G. Hadt, J. R. Sabin, G. Reina, P. Galloni, B. Floris, *Inorg. Chem.* **2010**, *49*, 7497–7509; f) V. N. Nemykin, G. T. Rohde, C. D. Barrett, R. G. Hadt, C. Bizzarri, P. Galloni, B. Floris, I. Nowik, R. H. Herber, A. G. Marrani, R. Zanoni, N. M. Loim, *J. Am. Chem. Soc.* **2009**, *131*, 14969–14978; g) U. Pfaff, A. Hildebrandt, D. Schaarschmidt, T. Hahn, S. Liebing, J. Kortus, H. Lang, *Organometallics* **2012**, *31*, 6761–6771.
- [24] D. E. Richardson, H. Taube, *Inorg. Chem.* **1981**, *20*, 1278–1285.
- [25] G. Gritzner, J. Kuta, *Pure Appl. Chem.* **1984**, *56*, 461–466.
- [26] M. Krejčík, M. Daněk, F. Hartl, *J. Electroanal. Chem.* **1991**, *317*, 179–187.
- [27] F. Paul, L. Toupet, J.-Y. Thépot, K. Costuas, J.-F. Halet, C. Lapinte, *Organometallics* **2005**, *24*, 5464–5478.
- [28] C. G. Atwood, W. E. Geiger, *J. Am. Chem. Soc.* **1994**, *116*, 10849–10850.
- [29] M. B. Robin, P. Day, *Adv. Inorg. Chem. Radiochem.* **1967**, *10*, 247–422.
- [30] F. Paul, L. Toupet, J.-Y. Thépot, K. Costuas, J.-F. Halet, C. Lapinte, *Organometallics* **2005**, *24*, 5464–5478.
- [31] H. B. Gray, Y. S. Sohn, N. Hendrickson, *J. Am. Chem. Soc.* **1971**, *93*, 3603–3612.
- [32] J. Polin, H. Schottenberger, *Org. Synth.* **1996**, *73*, 262–267.
- [33] C. Zonta, F. Fabris, O. De Lucchi, *Org. Lett.* **2005**, *7*, 1003–1006.
- [34] H. M. Gilow, D. E. Burton, *J. Org. Chem.* **1981**, *46*, 2221–2225.
- [35] H. C. Clark, A. B. Goel, *Inorg. Chim. Acta* **1978**, *31*, 441–442.
- [36] N. Miyaura, A. Suzuki, *Org. Synth.* **1990**, *68*, 130–132.
- [37] A. Nafady, W. E. Geiger, *Organometallics* **2008**, *27*, 5624–5631.
- [38] G. M. Sheldrick, *Acta Crystallogr., Sect. A* **1990**, *46*, 467–473.
- [39] G. M. Sheldrick, *Program for Crystal Structure Refinement*, University of Göttingen, Germany, **1997**.

Received: November 7, 2013

Published Online: January 15, 2014